Metal nanowire network as an efficient top electrode for Si solar cell

A thesis submitted in partial fulfillment for the degree of

Master of Science (M. S.)

as a part of the Integrated Ph. D. programme

(Materials Science)

by

Nikita Gupta

Chemistry and Physics of Materials Unit

Jawaharlal Nehru Centre for Advanced Scientific Research

A Deemed University, Bangalore, INDIA

March 2016

DEDICATED TO

MY PARENTS AND BROTHER

Declaration

I hereby declare that the thesis entitled "Metal nanowire network as an efficient top electrode for Si solar cell" is an authentic record of research work carried out by me at the Chemistry and Physics of Materials Unit, Jawaharlal Nehru Centre for Advanced Scientific Research, Bangalore, India under the supervision of Professor G. U. Kulkarni and that it has not been submitted elsewhere for the award of any degree or diploma.

I hereby certify that all of the work described within this thesis is the original work of the author. Thus going with the pre-existing practice of reporting scientific observations, due acknowledgement has been made whenever a work represented mentioned is based on the findings of other investigators. Any omission that might have occurred due to oversight or error in judgment is regretted.

_____

Nikita Gupta

31st March, 2016

Certificate

Certified that the work described in this thesis titled "*Metal nanowire network as an efficient top electrode for Si solar cell*" has been carried out by Ms. Nikita Gupta at the Chemistry and Physics of Materials Unit, Jawaharlal Nehru Centre for Advanced Scientific Research, Bangalore, India under my supervision and that it has not been submitted elsewhere for the award of any degree or diploma.

Professor G. U. Kulkarni

(Research Supervisor)

Acknowledgements

I express my heartfelt gratitude and immense admiration to my mentor and thesis supervisor Prof. G. U. Kulkarni. I sincerely thank him for providing me interesting research problems and guiding me at this early stage of research. He has always inspired me to perform better and unleash my full potential.

I thank Prof. C.N.R. Rao for his encouragement. His mere presence is a great source of inspiration.

I thank all the faculty members of JNCASR: Prof. Chandrabhas, Dr. Eswaramoorthy, Prof. K.S.Narayan, Prof. Shivaprasad, Dr. Sundareshan, Dr. Tapas Maji, Dr. Ranjan Dutta, Prof. Rajesh Ganapathy, Ass. Prof Subir K. Das, Prof. U. Waghmare, Dr. S.K. Pati, Dr. Balasubhramaniam and Prof. S. Narashiman for the courses that have been extremely beneficial.

I am grateful to Dr Mallik for supervising me in my MS work along with my guide and to all past and present lab mates for their cooperation, help in experiments, useful discussions and cheerful company. I would also like to thank Ms. Chaitali for providing SEM, fill factor and Raman data for the characterization of free standing Au mesh.

I thank Mr. Srinath, Mr. Srinivas and Mr. Srinivas Rao for the technical assistance. I acknowledge Sunil for timely help and friendly attitude. I am very thankful to Selvi (SEM), Dr. Basavraja (AFM), Mr. Anil (XRD) and Mr. Basu (UV and PL) for their constant help.

I thank the staff of academic and administrative section in JNC for their assistance. I also thank the library staff for their help. I am thankful to the computer lab staff. I thank DST for financial assistance.

I thank my CPMU and NCU batch mates for enjoyable company in and outside classroom, useful discussions, assignments, birthday treats and many more fun-filled moments.

I am grateful to Mrs. Indira Kulkarni for providing me homely atmosphere, warmth and care. I also thank Teju and Poorna for bringing some happy moments, fun and laughter.

I would like to give special thanks to Ms Aishwariya Iyyenger, Mr Abhiroop Lahiri, Ms Disha Bhange, Mr Amit Bhattacharya, Mr Uttam Gupta, Ms Shrimayee Mukherjee and my BSG friends who have been supportive in all situation.

I would like to conclude by extending my deepest gratitude to my family. Without their unconditional love and support, I would have not been able to complete this degree. I owe a lot to my family.

Preface

This thesis deals with optimization and fabrication of metal wire network as top electrodes for silicon substrates and as free standing transparent conductor.

Chapter 1 deals with introductory topics about transparent conductors and the challenges faced by these.

Chapter 2 lists the various experimental techniques used for fabrication and characterization in this study.

Chapter 3 describes the fabrication and optimization of metal wire network as top electrodes for Si solar cells. Three types of substrates have been chosen namely plain Si wafer, pristine corrugated Si solar cell and commercial Si solar cell. The chapter illustrates a thorough comparison of samples with and without metal network.

Chapter 4 discusses about ways to transfer as-prepared metal wire network on to various polymer substrates with aim of achieving flexible, transparent conductors. It also discusses the metal mesh which can freely stand and can be a transparent conductor all by itself.

Chapter 5 summarizes the results obtained from the study and gives brief future outlook of the thesis work.

Table of Contents

Chapter 1

Introduction

In optoelectronic applications, a transparent conductor plays a very important role. It allows photons as well as electricity to pass through, be it a situation involving a display device or an energy device. Accordingly, the requirements of transparent conducting electrodes (TCE) are highly varied. Display devices require TCEs with high transparency and moderate conductivity whereas energy devices necessitate high conductivity while moderate transparency is acceptable.

While tin (Sn) and fluorine (F) doped indium oxide (ITO and FTO respectively) are extensively used in various devices (T = 92% and Rs = 10Ω/□)[1], many alternate materials are being investigated to address the shortcomings in oxide based TCEs such as extreme brittleness, limited chemical stability, high cost etc. In this context, conducting 1D networks made of carbon nanotubes and silver nanowires have become popular. By bringing in dispersions of these 1D nanostructures and spreading over a given substrates, TCEs have been realised with transparency and sheet resistance comparable to that of ITO. However these percolative networks come with drawbacks such as high junction resistance and redundant wires causing undesired shorting in the device.

There have been efforts to make wire networks by lithography methods as well. Transparent grid patterns of desired size and shape has been recently developed for different applications. Recently, Al nanomesh thin films have been prepared by two step approach of direct anodic aluminium oxide wet etching treatment.[2] Recently, random nanostructured Au mesh was fabricated by employing grain boundary lithography.[3] Growth patterns of sodium carbonate crystals have also been used as template for the fabrication of silver metal network.[4] While lithography methods yield high quality holey films, the processes are not affordable and not easily scalable. While self-assembly processes produce such structures for limited areas, ensuring continuity over large area is rather difficult with such processes. On the

other hand, recently graphene has emerged as one of the key candidates to replace ITO based TCEs with excellent transparency (97%) and sheet resistance (100 – 30 Ω/□).[5] However it demands careful and intensive instrumentation for large area fabrication.

Recently, in this laboratory a templated method has been attempted using a colloidal dispersion which upon drying produces interconnected fine cracks in the film.[6] The cracked layer is used as a template to fill in metal either by physical or chemical methods. Thus produced networks are found to be highly conducting and transmitting. The present work employs crack templating method directly applied to a silicon (Si) solar cell, importantly going well with its complex architectures.

References:

1. Wang, S.; Zhang, X.; Zhao, W., Flexible, Transparent, and Conductive Film Based on Random Networks of Ag Nanowires. *Journal of Nanomaterials* **2013,** *2013*, 6.
2. Li, Y.; Chen, Y.; Qiu, M.; Yu, H.; Zhang, X.; Sun, X. W.; Chen, R., Preparation of Aluminum Nanomesh Thin Films from an Anodic Aluminum Oxide Template as Transparent Conductive Electrodes. *Sci Rep-Uk* **2016,** *6*, 20114.
3. Guo, C. F.; Sun, T.; Liu, Q.; Suo, Z.; Ren, Z., Highly stretchable and transparent nanomesh electrodes made by grain boundary lithography. *Nat Commun* **2014,** *5*.
4. Lee, D. E.; Go, S.; Hwang, G.; Chin, B. D.; Lee, D. H., Two-Dimensional Micropatterns via Crystal Growth of Na2CO3 for Fabrication of Transparent Electrodes. *Langmuir* **2013,** *29* (39), 12259-12265.
5. Kumar, R.; Mehta, B. R.; Bhatnagar, M.; S, R.; Mahapatra, S.; Salkalachen, S.; Jhawar, P., Graphene as a transparent conducting and surface field layer in planar Si solar cells. *Nanoscale Res Lett* **2014,** *9* (1), 349-349.
6. Rao, K. D. M.; Gupta, R.; Kulkarni, G. U., Fabrication of Large Area, High-Performance, Transparent Conducting Electrodes Using a Spontaneously Formed Crackle Network as Template. *Adv Mater Interfaces* **2014,** *1* (6).

Chapter 2

Experimental Methods

Several microscopic and spectroscopic techniques have been used to characterize the samples reported in this thesis. In the following paragraphs, the details of instruments used and the sample preparation methods are described.

Scanning electron microscope (SEM): Scanning electron microscopy (SEM) measurements were performed using a Nova NanoSEM 600 equipment (FEI Co., The Netherlands).

Energy dispersive spectroscopic (EDS): EDS mapping was performed using EDAX Genesis V4.52 (USA) attached to the SEM column. The EDS mapping was performed at 10 kV (energy window, 10 eV) with a beam current of 1.1 nA.

Optical profiler: For film thickness measurements, a Wyko NT9100 (Veeco, USA) optical profiler (OP) was used. In OP, the vertical scanning interferometry (VSI) for roughness of samples more than 160 nm and phase shifting interferometry (PSI) mode for roughness of samples less than 160 nm were employed with a field of view and objective lens magnifications from 0.5x – 2x and 5x – 50x respectively.

Optical and dark field microscope: The optical images were procured with the microscope of Laben, India with a zoom-in lens of 100x. The images were captured using IS capture software. IM-20 BD inverted Bright Field/ Dark field microscope was used to capture images for better clarity of the samples.

X-ray photoelectron spectroscopy (XPS): X-ray photoelectron spectroscopy (XPS) was carried out with OMICRON spectrophotometer ($1x10^{-10}$ Torr vacuum) with nonchromatic X-ray source of Al Kα (E =1486.6 eV). Samples for XPS (solid substrates) were mounted on the stub using high vacuum compatible Ag paint and drying in a vacuum.

UV-Vis and IR: UV-visible spectra were recorded using a Perkin-Elmer Lambda 900 UV/vis/NIR spectrophotometer. The photoluminescence (PL) spectra were taken

with different excitation wavelength from the spectroflurometer. PL was measured on Perkin- Elmer LS55 Luminescence spectrometer. Fourier transform infrared (FTIR) measurements were done using a Bruker IFS66v/s spectrometer with a resolution of ~ 2 cm^{-1}.

Solar simulator: Solar Simulator model SS50AAA-GB was used to create artificial sunlight (AM 1.5) for solar cell characterization. All the J-V measurements were performed by Keithley 2400 setup.

LBIC: The Laser Beam Induced Current Mapping experiments were carried out at DTU using a custom made setup with 410 nm laser diode (5 mW output power, 100 µm spot size ~65 W/cm^2, ThorLabs) mounted on a computer controlled XY-stage. A custom written computer program was used to scan the substrate in a raster pattern in 200 µm steps in the X and the Y directions, logging the coordinates and measured current.

Chapter 3

Metal nanowire network as an efficient top electrode for Si solar cell

Introduction

Laying current collecting electrodes on Si solar cells has been a topic of research for decades. Conventionally a Si solar cell employs a silver busbar and fine silver fingers perpendicular to the busbar as the top electrode on the light-incident side. For efficient light absorption, maximum area of silicon should be exposed hence demanding low coverage by the silver grid lines. On the other hand, for effective collection of photogenerated charge carriers, the silver grid lines should have closely spaced fingers necessitating its high coverage. Therefore, for conventional Si solar cells, high charge collection is possible only at the cost of reduced generation of light induced carriers hence putting a limit to enhancing the efficiency of these cells. As we know, silver has lowest resistivity among metals (1.59×10^{-6} Ωcm), silver nanowire exhibit high electrical conductivity maintaining comparable transparency. Carbon nanotubes[1] and graphene[2] have also come up as alternative top transparent electrodes but their electrical conductivity is lower than metal nanowires. However, these techniques suffer from the major issue of contacting the active layer via antireflection and surface passivation layers without significant shadowing. Several approaches like optimization of interfacial layer formation, three dimensional (3D) nanowire structures for light trapping and antireflecting properties[3] have been attempted to improve the efficiency of Si solar cells. In present work, indigenously developed crackle lithography has been employed to fabricate top electrodes on Si wafer, corrugated p-n junction silicon solar cells and commercially available Si solar cells with antireflection and silver grid lines on top.

Experimental Section

(a) Fabrication of crack template

Plain Si wafer and Si solar cell, both were cleaned by ultra-sonication in acetone, IPA, DI water consecutively. To introduce the crackle template, 0.7 mg/µL crackle precursor (CP) was spin coated on each substrate.

(b) Physical Deposition of Metal on crack template

Resistive evaporation of metals like Sn, Ag, Ni onto the CP patterned Si substrate was done using a thin film deposition system (HindHi Vac., Bangalore) at a base pressure of 1×10^{-6} torr. The substrate was held directly facing the tungsten basket containing metal fillings, at a distance of ~12.5 cm. Lift-off of the crack template was carried out in chloroform (5 min). The patterned substrates were examined using a Nova NanoSEM 600 instrument (FEI Co., The Netherlands) and Optical Microscope (Laben, India). The optical reflectance was measured in the diffused mode using Perkin-Elmer Lambda 900 UV/visible/near-IR spectrophotometer.

(c) Electroless Deposition of Metal on crack template

Au electroless solution (10mM) was prepared by dissolving 17 mg $HAuCl_4$, 1.1 mL HF in 3.9 mL DI water. Ni electroless solution was prepared by dissolving 3 g Nickel Chloride, 2 g Sodium Hypophosphite, 6.5 g Triammonium citrate in water.[4] This solution was mixed with Ammonium Hydroxide in the ratio 20:1 at 70 °C. Cu electroless deposition was performed by dipping Ni coated solar cell in 10:1 (v/v) solution of Cu A and Cu B. Cu A was composed of 3 g $CuSO_4$, 14 g of Sodium potassium tartarate and 4 g NaOH in 100 ml DI water. Cu B is formaldehyde.[5] After metal deposition, the crack template was removed by lifting it off in chloroform and further rinsing by IPA.

(d) J-V measurements

The electrical connections were made using Ag paste on the top and bottom of the cell with Cu wires to make circuit connections. Top Ag contact was made square shaped. The device was connected to Keithley 2400 setup for IV measurement. All the measurements were performed in ambient conditions under AM 1.5 illumination using Solar Simulator model SS50AAA-GB.

(e) Laser beam induced current mapping (LBIC)

The LBIC experiments were carried out at DTU using a custom made setup with 410 nm laser diode (5 mW output power, 100 µm spot size ~65 W/cm^2, ThorLabs) mounted on a computer controlled XY-stage. A custom written computer program was used to scan the Au wire Si network in a raster pattern in 200 µm steps in the X and the Y directions, logging the coordinates and measured current. The results were then converted to yellow/blue colored bitmaps in 255 different hues with another custom written program. Bright yellow represents the highest absolute current extracted while blue represents the lowest current. Current profiles along selected directions were taken from these maps to visualize the relative differences in different regions.

Part I. Silicon wafer

I.1 Fabrication and characterization of metal wire elecrode on Si

Silicon wafer readily gives gold films at room temperature by electroless deposition. Using crackle lithography technique, Au wire network is grown electrolessly on Si wafer. A colloidal crackle precursor (CP) is spin coated on a polished n-type (100) oriented Si substrate, as depicted in Figure 3.1a. The Si substrate exposed in between the cracks provides an active site for the electroless deposition of Au. The Si substrate carrying crack template was dip in Au plating

solution (10 mM $HAuCl_4$ with 2%HF) for 30 s resulting in deposition of Au metal in the crackle groove. The deposition process and the expected reaction that takes place on the Si surface in presence of Au precursor and HF is shown schematically in Figure 3.1b. The Au nanoparticles nucleate, coalesce and grow in between the cracks as long as the surface of Si is completely covered. The deposition time of 30 s resulted in interconnected Au network. After the Au deposition, the crackle template was

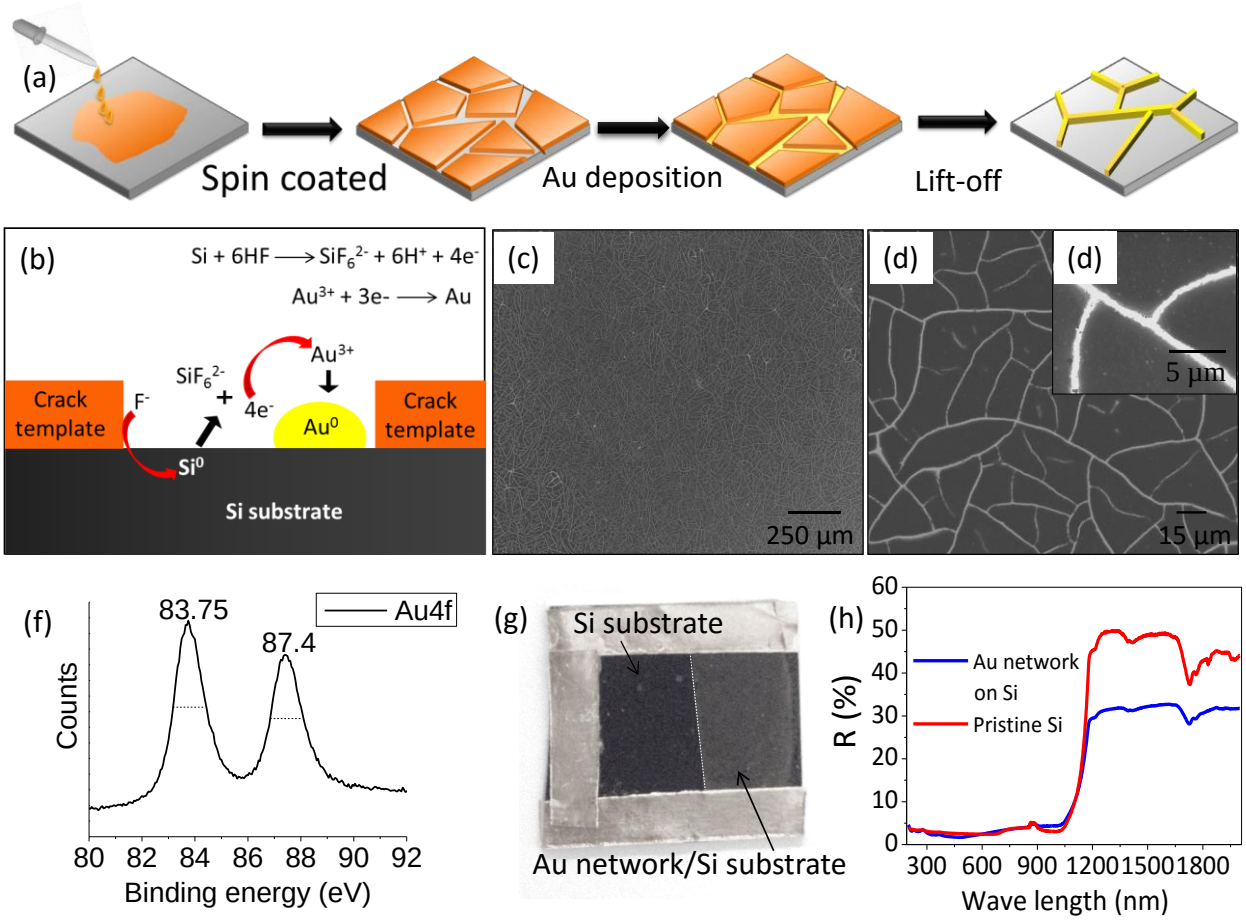

Figure 3.1 (a) Schematic demonstration of the steps involved in the fabrication of Au wire network on Si substrate following crack template method. (b) Mechanism for reduction of Au on Si exposed from the crackle grooves. SEM images of Au wire network (c) showing the bird eye view over large area (1.8 x 1.5 mm^2), (d) and (e) are magnified view. (f) XPS spectra for Au 4f signal. (g) Photograph of Si substrate partially covered with Au network (h) Reflectance spectra for pristine Si and Au wire network on Si.

removed by washing in chloroform, forming a continuous wire network of Au (Figure 3.1c) uniformly spread over 1.8 × 1.5 mm^2 area. The metal fill factor

(percentage area coverage) was calculated to be ~ 12% and cell size of 15 - 30 µm (Figure 3.1d). The Au wire network is continuous from one end of the substrate to the other end. Figure 3.1e depicts magnified view of one strand of Au wire network, which is ~ 0.7 µm in width and ~ 90 nm in thickness with very good particle interconnectivity. Indeed, the junction between the wires is seamless, leading to almost negligible junction resistance. Since Au is electrolessly deposited on Si substrate, its surface was further analyzed by XPS studies. The Au $4f_{7/2}$ and $4f_{5/2}$ peaks are located at 83.75 and 87.40 eV respectively indicating the presence of metallic gold. Sharpness of the peaks again indicates metallic nature of gold. In order

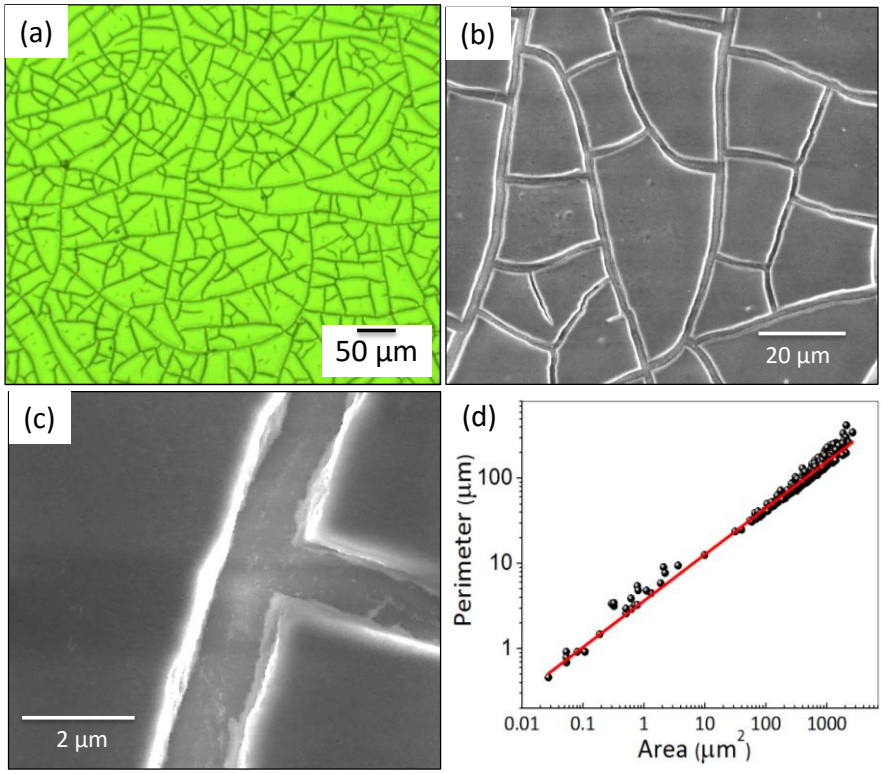

Figure 3.2 (a) Optical micrograph and (b) SEM image of crackle pattern. (c) A magnified view of a single crackle. (d) log-log plot between perimeter and area of the crackle network calculated from (a).

to determine the optical properties of patterned Si (Si/Au network), reflectance measurements were carried out along with that for pristine Si substrate in a broad spectral range. The reflectivity is nearly similar for both the substrates in the UV-vis

range of 380 to 900 nm. Interestingly, the reflectance of Si/Au network substrate is ~ 12 – 15% less (see Figure 3.1h) in a broad IR spectral range from 1200 to 2000 nm compared with pristine Si substrate. This indicates that the Au wire network acts as an antireflective coating on Si substrate in addition to serving as a current collecting grid.

The microscopy analysis of crack formation is described in Figure 3.2. The micro-crack pattern form spontaneously upon drying without any external stimuli. The crackles start from one end of the substrate and ends on the other end, virtually limited by substrate area. Indeed, the crackle film consists of islands of squares, triangles and polygons clearly seen by the optical micrograph in Figure 3.2a. The scanning electron microscopy (SEM) image of the crackle patterns given in Figure 3.2b shows high interconnectivity of cracks with each other which is crucial for electrode fabrication. More importantly, the crackles form down to Si substrate without any residual layers depicted by high magnification SEM image in Figure 3.2c. This is essential for usage of the crackled film as a template for patterning. Interestingly, the cracks are much narrower in width compared to the cracks on PET, quartz and glass substrates as observed in previous studies.[6] The perimeter versus area of the crackle network follows power law (see figure 3.2d). Fractal dimension of the network was calculated to be 1.08 by box method. This indicates the Au wires are straight with minimal curvature[7].

I.2 Photo response of Si/Au network

The current collection efficiency of Au wire network was examined by measuring the responsivity of pristine Si and Si/Au network. Figure 3.3a shows the

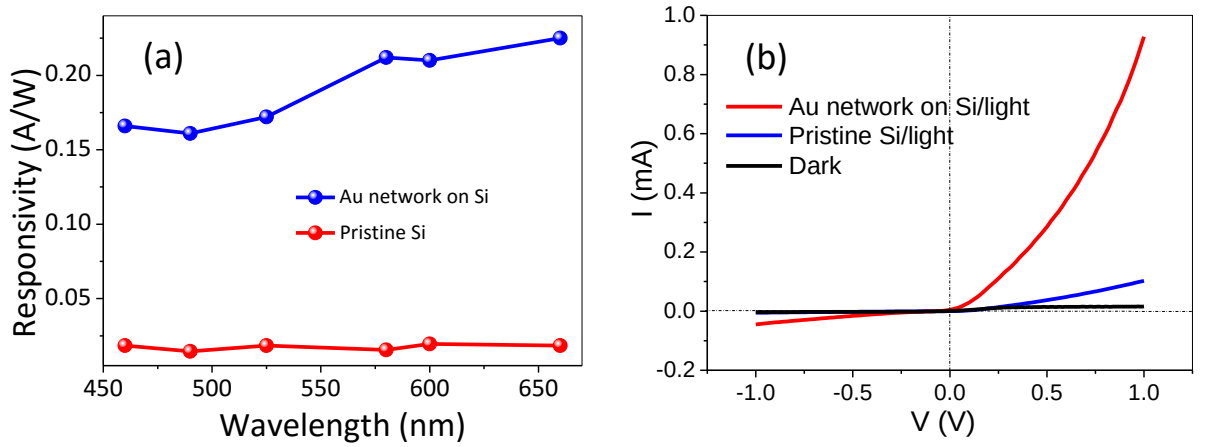

Figure 3.3 (a) Responsivity of pristine and patterned Si as a function of wavelength. (b) I-V characteristics of Si with and without Au network in light and in dark. Note that the dark current and light current for pristine Si is multiplied by a factor of 2 for better visibility.

DC responsivity of Au wire network on Si substrate at 3 V in the visible range from 460 to 660 nm. As seen from the plot, photoresponse of Au wire on Si is lower (0.16 A/W) in the blue region (460 nm) compared to green (530 nm; 0.176A/W) and red regions (650 nm; 0.222 A/W). This is due to the inherent nature of absorption of Si. Comparatively, the photoresponse from Si alone appears to be rather flat due to increased recombination of photogenerated charge carriers in absence of current collecting grid. The average photoresponse of the Au wire carrying Si substrate is 0.19±0.03 A/W, which is one order higher compared to pristine Si substrate. The photoresponse of Si/Au network is measured under white light and can be seen from the I-V characteristics in Figure 3.2b. The overall photocurrent is one order higher in magnitude with respect to the dark current. The Si/Au network substrate is collecting more photocurrent due to presence of collecting grid leading to increase in the responsivity and photocurrent.

I.3 Laser Beam Induced Current Mapping on Si/Au network

The laser beam induced current mapping is done to study the relative current extraction from the Si substrate upon introduction of Au metal network as current collecting grid shown schematically in Figure 3.4a. The optical images of Au wire

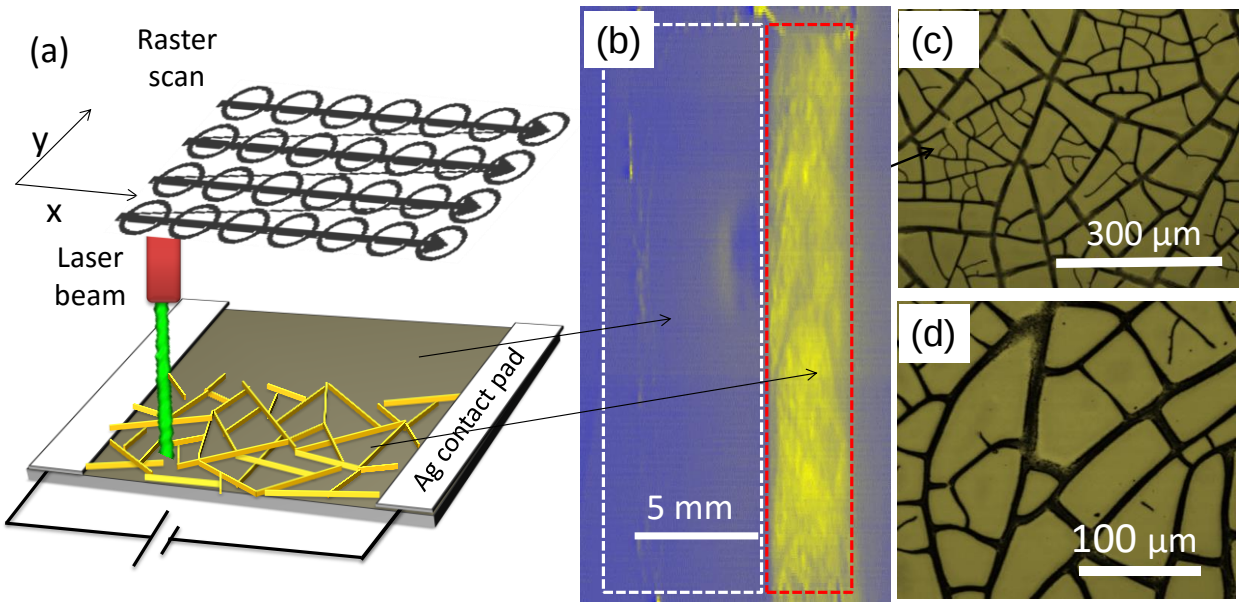

Figure 3.4 (a) Schematic showing raster scanning by laser over Si/Au network device for Laser Beam Induced Current (LBIC) experiment. (b) LBIC map where area with and without Au network is shown by rectangles with red and white dotted lines respectively. (c,d) Optical images of Au network on Si substrate at different magnifications.

network formed on Si substrate is shown in Figure 3.4c and d and the corresponding measured photocurrent map (LBIC) over large area window is depicted in Figure 3.4b. The LBIC map was characterized by the yellow and blue color levels where complete blue region corresponds to zero photocurrent and bright yellow region corresponds to high photocurrent. The pristine area on Si and Au wire containing region are clearly demarcated by white and red dotted rectangles in Figure 3.4b. The uniform yellow region indicates that the photocurrent is uniform across the whole area without any defects or shadowing loss due to Au wire network geometry.

Part II. Ŝi solar cell

Corrugated Si solar cell without SiN_x passivation or screen printed Ag electrodes, henceforth termed as Ŝi solar cell is a complex architecture both structurally and chemically compared to a polished Si wafer. The pyramidal corrugation of the top surface is purposefully designed as an antireflection layer to harvest more photons for charge carrier production. Here, an attempt has been made to study how different metal wire networks behave given the corrugated nature of the surface.

II.1 Ŝi solar cell/ Au-Cu network

Getting inspired by the photoresponse of Au wire network on polished Si wafer, Ŝi solar cell was coated with Au network. Initially, Ŝi solar cell was cleaned by ultra-sonication in Acetone, IPA and deionized (DI) water and then a crackled film was brought on top by spin coating CP as done for polished Si wafer. Au was deposited in the cracks by sputtering and in order to decrease the resistance of the top wire network, Cu was deposited on Au as a seed layer by electro-less deposition.

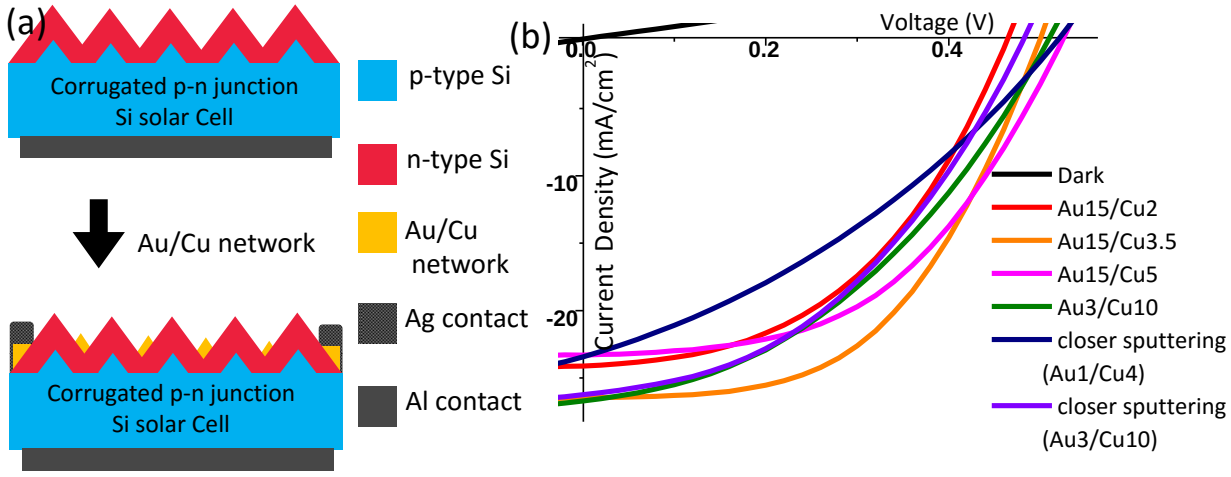

Figure 3.5 (a) Side view schematic of Ŝi solar cell before and after coating with Ni wire network by physical/electroless deposition (b) Zoom in view of J-V characteristics of Ŝi solar cell/ Au-Cu network under varying conditions compared with dark.

The side view schematic in Figure 3.5a shows Ŝi solar cell before and after coating Au/Cu wire network. As can be seen in Figure 3.5b, varying the deposition time of Au/Cu network, the J-V characteristics got influenced. Sputtering of Au for 15 minutes from a distance of 16 cm from the source and performing Cu electroless deposition for 3.5 minutes (Au15/Cu3.5) found to be the optimum thickness for Au/Cu network and gave maximum efficiency of 6.89%. The deposition of Au15/Cu5 was little less efficient (6.00%) than Au15/Cu3.5. This might be due to higher aspect ratio of Au/Cu wire network at higher Cu deposition which gives rise to higher reflection. The higher reflection caused lesser absorption of incident light in turn reducing the overall current density in the sample. On the other hand, less Cu deposition as in case of Au15/Cu2 decreased the open circuit voltage (V_{oc}). Sputtering Au from closer distance (8 cm) for different deposition times leads to decrease in the Fill Factor (FF) of the J-V curve. The high sputtering heat due to closer distance is expected to have caused damage to crystallinity of the sample. As sputtering technique is known to deposit metal deep into the target, there could have been plenty of places where Au has shorted the p-n junction leading to poor shunt resistance. It was observed that sputtering away from the target gave better squareness of J-V curve.

As can be seen from the SEM images in Figure 3.6, the Au network is deposited uniformly over the solar cell which helps in current collection with low recombination losses. The wire network is free of any junction resistance unlike in case of carbon nano-tubes (CNTs) and silver nanorods. It sits conformally onto pyramidally textured surface of Silicon thereby reducing series resistance. These unique features of crackle network makes the fabricated solar cell stand out from its counterparts.

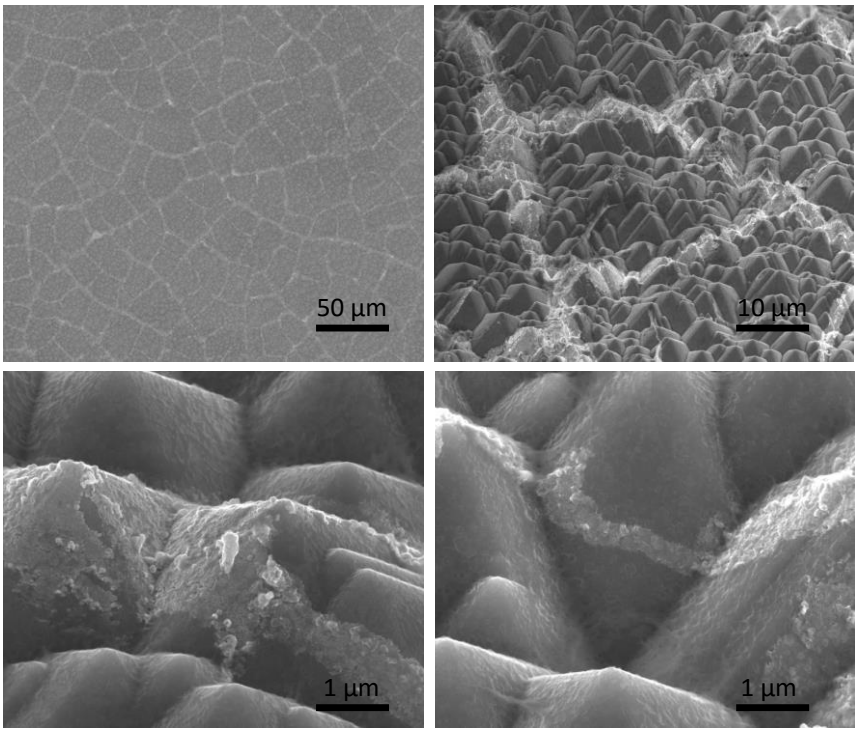

Figure 3.6 SEM images for Ŝi solar cell/Au-Cu network at different magnifications.

.

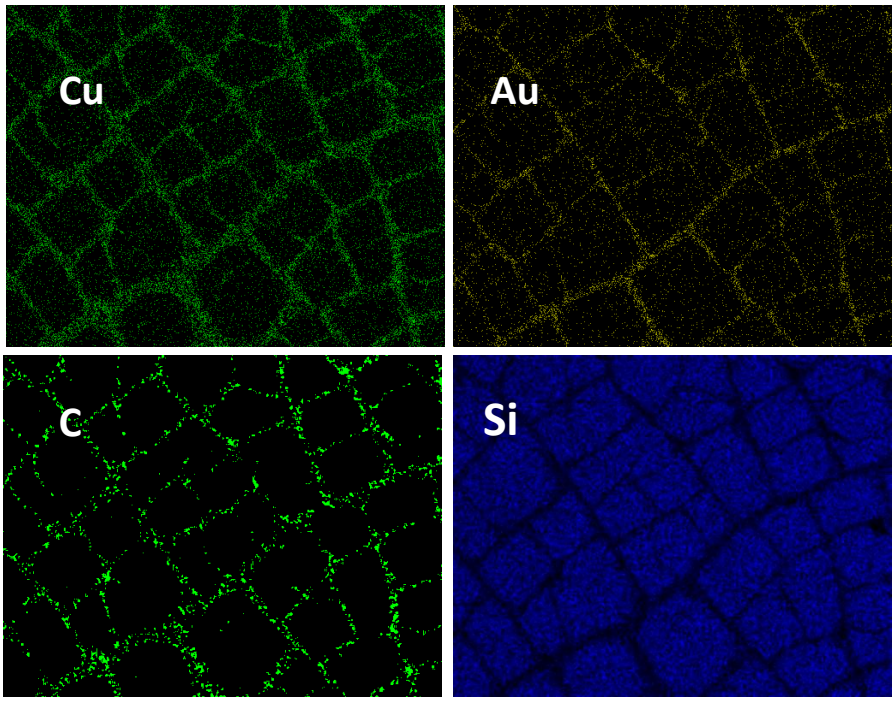

Figure 3.7 EDS mapping of Cu, Au, C and Si on Ŝi solar cell/Au-Cu network

Energy dispersive x-ray spectroscopy (EDS) mapping was performed on a region of Ŝi solar cell/Au-Cu network as shown in Figure 3.7. The spread of Cu is found to be more than Au since it deposited beneath Cu. Some carbon is also present in crackle regions. The reason for this might be the presence of organic impurities in electroless solution. The absence of Carbon in regions other than cracks suggest complete lift off of crackle precursor. The signal of Si in the cracks is observed to be very less due to high thickness of Au-Cu on it.

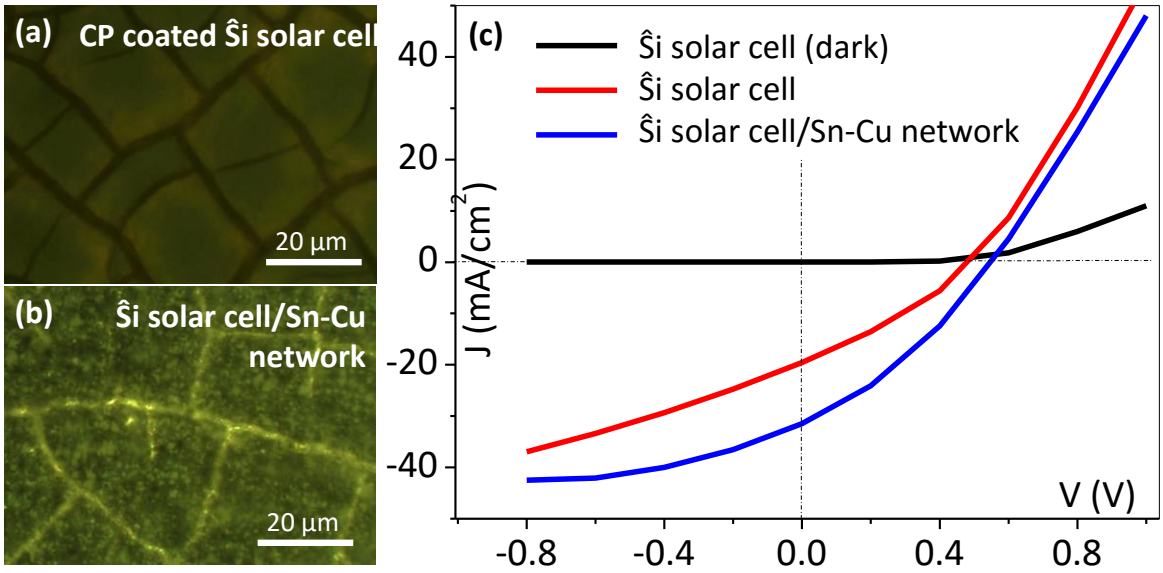

Figure 3.8 Optical micrographs of (a) CP coated on Ŝi cell, (b) Ŝi solar cell/Sn-Cu network. (c) J-V charcteristics of Ŝi solar cell with and without Sn-Cu network compared with dark.

II.2 Ŝi solar cell/ Sn-Cu network

As gold is very expensive, cheaper metal like tin (Sn) is explored as a seed layer for Cu in the following work. Specifically Sn is chosen as it is known to be a low melting solid thereby giving a possibility of its soldering action on annealing. The Ŝi solar cell with crackle template (Figure 3.8a) is deposited thermally with Sn. Over this Cu electroless deposition is performed for 3 minutes followed by CP lift off in chloroform. The Optical micrographs for Ŝi solar cell coated with Sn-Cu wire network (Ŝi solar cell/Sn-Cu network) are shown in the Figure 3.8b.

J-V characteristics was measured before and after putting Sn/Cu wire network (see Figure 3.8c). After putting the wire network, 5.88% efficiency was achieved compared to 2.89% in pristine sample. It is known that V_{oc} is directly related to recombination process. We can observe that here the V_{oc} of the solar cell increases because by putting wire network, the collection of charge carriers becomes easier and the recombination gets reduced.

Table 3.1. Solar cell parameters for Ŝi/Sn-Cu network solar cell compared with before and after annealing and pristine.

	Ŝi	Ŝi/Sn-Cu network	Ŝi/Sn-Cu network (10 days kept in air)	Ŝi/Sn-Cu network (Annealed for ½ h)
Area (cm^2)	4.3	4.3	4.3	4.3
Voc(V)	0.478	0.546	0.53	0.48
Jsc (mA/cm^2)	-19.58	-31.50	-22.55	-11.16
Efficiency (%)	2.89	5.88	4.25	1.45
Fill Factor	31.07	34.16	35.61	27.16

The efficiency of the same sample when kept in air for 10 days reduced to 4.25% (see Table 3.1). The possible reason for the deteriorated performance is oxidation of top layer of Cu in ambient atmosphere. This sample is then heated to 250 °C (melting point of Sn is 232 °C) for ½ h in Ar atmosphere in a glove box. Unlike as expected, the heating instead of annealing and making the contacts better, actually destroys the silicon sample beneath and the efficiency reduces considerably to 1.45%.

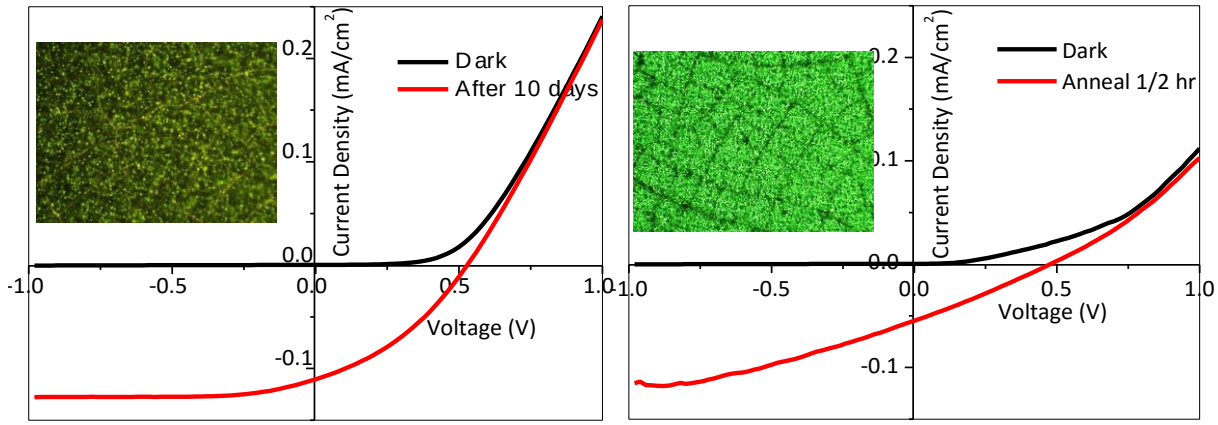

Figure 3.9 J-V characteristics of Ŝi solar cell/Sn-Cu network (a) before annealing, (b) after annealing in glove box at 250°C.

The J-V characteristics of Sn/Cu network coated cell before and after annealing is shown in Figure 3.9a and b along with optical micrographs at same scale.

II.3 Ŝi solar cell/Ni-Cu network

Due to annealing studies done on Ŝi solar cell/Sn-Cu network, there was an indication that either Sn or Cu is not good for silicon. As it is known from the literature that Au and Cu are not ideal metals to be used as electrodes for Si solar cells due to their diffusion into Si with time, a material was required which does not diffuse in to Si or a barrier is formed for the top Cu conducting layer to prevent this diffusion. Nickel is known to form silicide (Ni_2S) when it is annealed with silicon at temperature around 420°C. It is expected that the Ni_2S layer would form highly adhering contacts with Si. The Silicide would also prevent the top Cu conducting layer from diffusing into the Si solar cell and hence make it more stable. [8]

Before performing experiments with Ni, Ŝi solar cells were obtained from new source. Hence forth, the solar cell from new source is called Ŝi solar cell 2 and old source is called Ŝi solar cell 1. The details have not been disclosed for confidentiality purpose. Figure 3.10a and b show the optical micrograph of Ŝi solar cells 1 and 2 respectively. The corrugation appears to have smaller feature size in the Ŝi solar cell 1 compared to Ŝi solar cell 2.

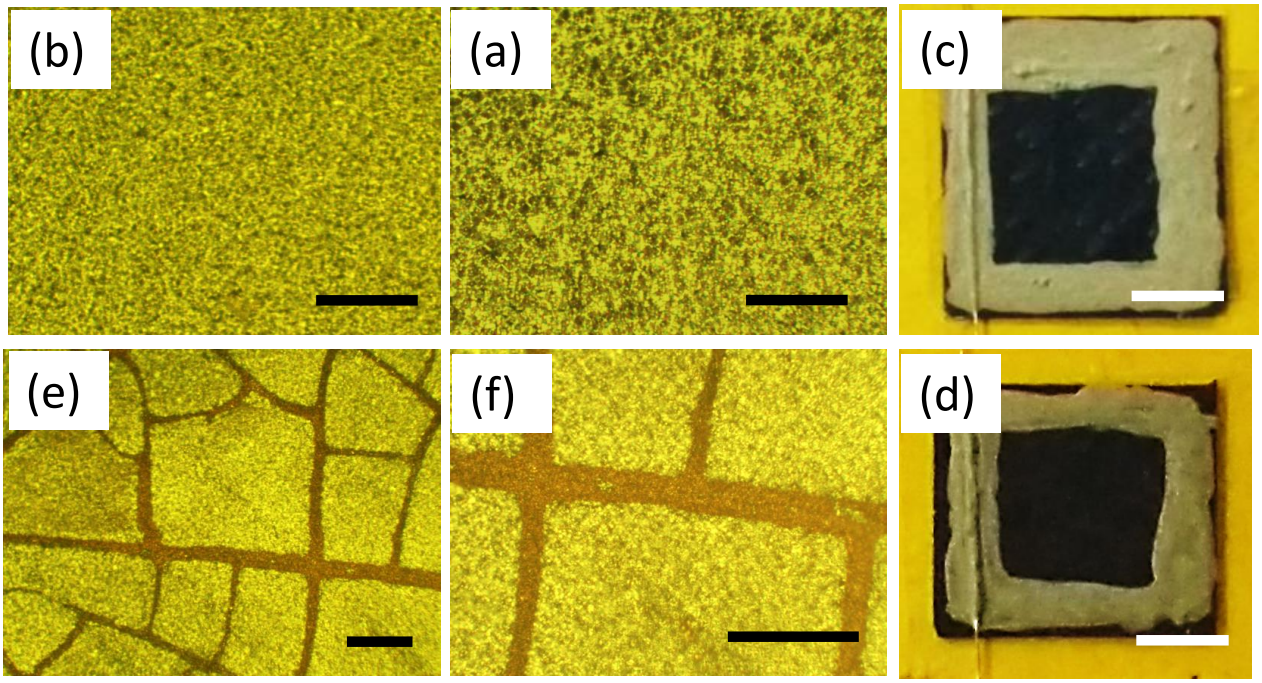

Figure 3.10 Optical micrographs of Ŝi solar cell from (a) source 1 and (b) source 2. (c) Digital photograph of Ŝi solar cell device with square Ag contacts and Cu wire attached on one side. (d, e) Optical micrographs of Ni-Cu network coated Ŝi solar cell in different magnifications. (f)Digital photograph of Ni-Cu network coated Ŝi solar cell device with square Ag contacts and Cu wire attached on one side. Black and white scale bars indicate 100 µm and 5 mm respectively.

Ŝi solar cell was cleaned and spin coated with CP in similar way as done previously. A 1%HF etch was performed to remove native oxide layer before CP coating. Ni was deposited by thermal evaporation to form a seed layer after which the CP was lifted off in chloroform. The substrate was annealed at 420 °C for varying durations to form Nickel Silicide (Ni_2Si) at the interface followed by Cu deposition on it by electroless plating (method given in experimental section). The CP was removed before annealing because it is not stable at higher temperatures and can char. Top and bottom contacts were made using Ag paste and Cu wires for both pristine and network coated samples (see Figure 3.10c and d). Figure 3.10e and f show Ni-Cu wire coated on Ŝi solar cell 2.

Table 3.2. Performance parameters of Ŝi solar cell without Ag and SiN_x before and after Ni electroless depositions.

Solar cell #	Pristine1	1	2	Pristine2	3	4	5	6
Source	1	1	1	2	2	2	2	2
Anneal time (s)	-----	30	5	-----	120	30	10	5
Cu Electroless time (min)	-----	10	10	-----	10	6	13.5	10
Area (cm^2)	4.68	1.78	0.42	2.4	1.69	0.77	1.8	0.81
V_{oc} (V)	0.54	0.54	0.54	0.51	0.51	0.49	0.55	0.54
J_{sc} (mA/cm^2)	16.97	21.03	33.73	7.23	19.80	28.29	23.32	24.35
FF (%)	36.33	48.85	57.95	20.67	32.68	42.85	48.68	51.42
Efficiency (%)	3.54	5.56	10.50	0.77	3.35	5.96	6.22	6.70

It was observed that solar cells from the two sources performed differently. Efficiency in pristine Ŝi solar cell 2 was only 0.77% compared to 3.54% in Ŝi solar cell 1. The performance of Ŝi solar cell from both the sources improved tremendously after bringing Ni-Cu wire network on top. Due to higher efficiency in the pristine Ŝi solar cell 1, it gives better performance after coating Ni-Cu network with the best one having an efficiency of 10.5%. As the annealing time for silicidation decreases, the efficiency monotonically improves for both types of cells (see Table 10.2). Figure 3.11a and b shows the J-V characteristics of Ŝi solar cell/Ni-Cu network for different annealing times from both the sources compared with their pristine samples. The annealing time study suggests that silicide formation takes only 5 sec and more annealing slowly deteriorates the device worsening its performance. It can be

concluded from the observed data that bringing Ni-Cu wire network always improves the efficiency of Ŝi solar cell irrespective of its quality. This is possible due to formation of channel for current collection.

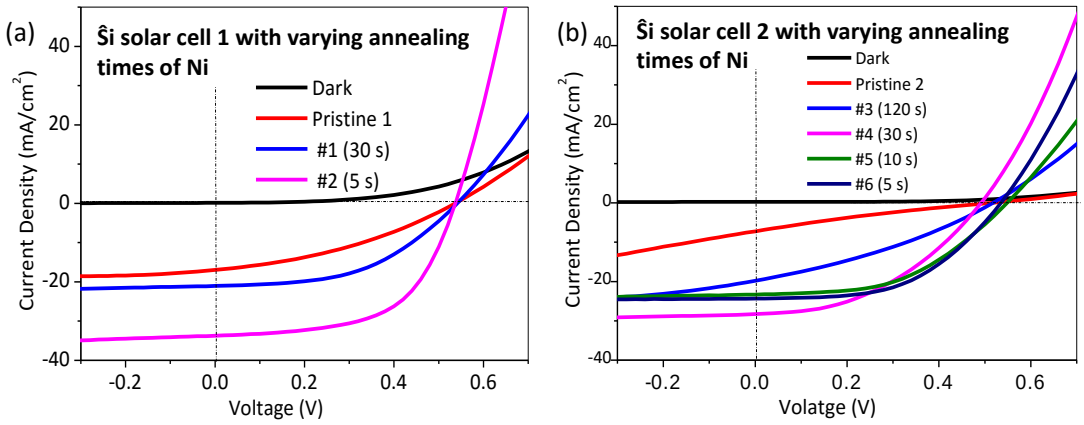

Figure 3.11 J-V characteristics of (a) Ŝi solar cell 1/Ni-Cu network and (b) Ŝi solar cell 2/Ni-Cu network with varying annealing times of Ni compared to pristine and dark.

II.4 Ŝi solar cell/Ni network

Nickel metal network can be grown conveniently by electroless technique at 70 °C in an aqueous solution of nickel chloride, tri-ammonium citrate and sodium hypophosphite by maintaining a pH around 8. The pH control was done by using ammonia water and a pH paper. The etching of top oxide coating on Ŝi solar cell was done similar to that done for thermal deposition. It allows Ni to nucleate on the Si surface easily. The inherent voltage of p-n junction of the solar cell aids the electroless deposition on Si. Performing silicidation of electrolessly grown Ni by annealing is not as effective as for thermally grown Ni network. Therefore, no Cu top conducting layer is deposited over electrolessly grown Ni and higher thickness of Ni is deposited by increasing deposition time to ensure good conductivity.

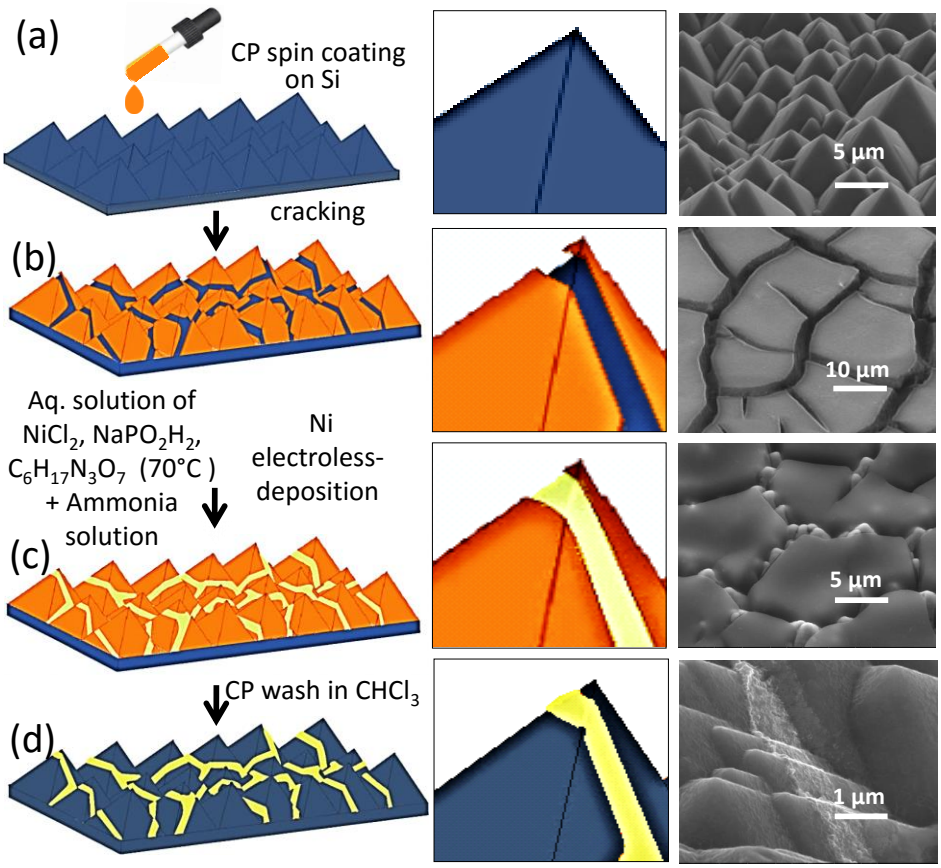

Figure 3.12 Fabrication of top electrode on Si solar cell (a-d) Schematic showing steps involved in the fabrication with a magnified view along with SEM images corresponding to each step. (a) Drop coating crackle precursor to get crack pattern on pristine Si solar cell. (b) Formation of cracks on corrugated surface of Si solar cell. (c) Deposition of Ni by electroless process. (d) Conformally coated Ni wire network on Si solar cell after washing in $CHCl_3$. Middle column is the zoomed-in view of left column for better depth visualisation of crack. Right column is the corresponding SEM image.

The SEM image in Figure 3.12a shows the high roughness of pyramidal corrugation on the solar cell. CP is coated on it similar to the previous cells (Figure 3.12b) and it forms cracks irrespective of the roughness. The as-prepared CP coated Si solar cell dissolves in the Ni electroless solution within 30 s. Therefore, the CP template was prebaked at 100 °C for 5 minutes to adhere better to the Si surface.

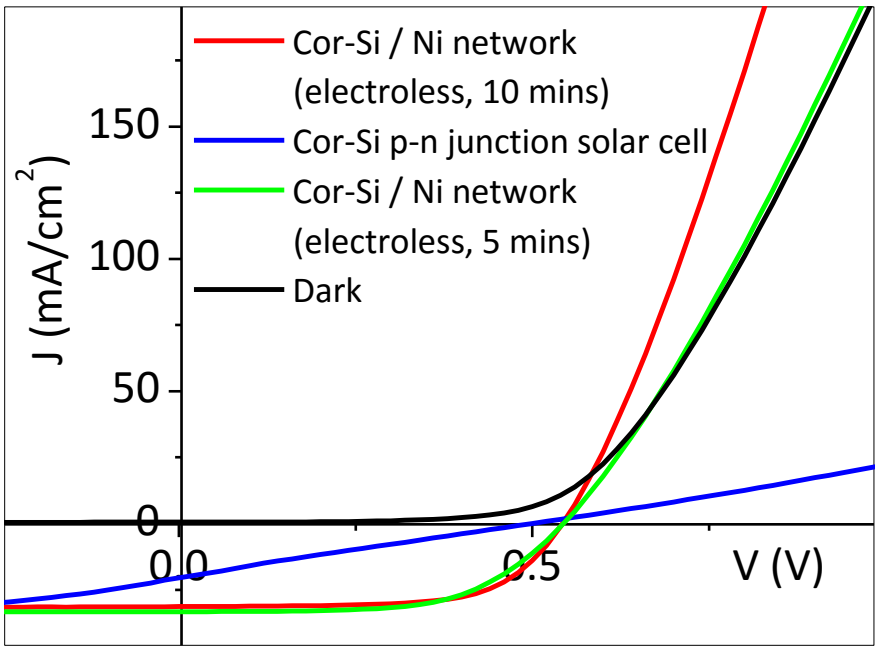

Figure 3.13 J-V characteristics of Ŝi solar cell before and after depositing Ni network with varying deposition duration and compared to dark.

The metal deposition on the exposed corrugated region can be clearly seen from the SEM image in Figure 3.12c. The small spheres in the crackle regions are due to deposition at the top of pyramids. After dissolving the crackle resin, Ni wire network was obtained on the top surface of Si solar cell. The network was strikingly found to sit conformally on the pyramidally corrugated Si surface as clearly seen by SEM image in Figure 3.12d. For Ni network grown on Ŝi solar cell (Ŝi solar cell/Ni network), Ni deposition was performed for different durations, J-V characteristics for which are shown in Figure 3.13. 10 minutes electroless deposition of Ni gives higher efficiency (11.15%) compared to 5 minutes deposition (10.85) (see Table 3.3). It is likely that the higher deposition time increases the conductivity and hence more effectively carries current.

Table 3.3 Performance parameters of Ŝi solar cell before and after Ni electroless deposition with varying deposition time of Ni.

Si Solar cell (without Ag and SiN_x)	Before Ni wire network deposition	After Ni wire network deposition (electroless)	
Prebake time (mins)	------	5	5
Ni electroless time (mins)	-----	5	10
Area (cm^2)	0.64	0.64	0.56
V_{oc}(V)	0.5	0.54	0.54
J_{sc} (mA/cm^2)	20.53	33.28	31.4
FF (%)	23.8	59.9	65.45
Efficiency (%)	2.79	10.85	11.15

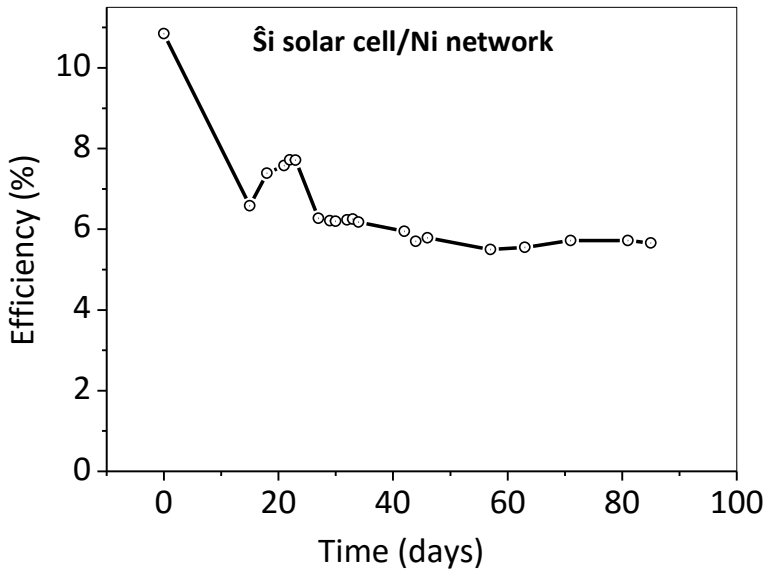

Figure 3.14 Aging of Ŝi solar cell/Ni network. Efficiency of corrugated p-n junction Si solar cell with Ni wire network plotted with time.

Fifteen days after preparing Ŝi solar cell/Ni network, the efficiency of the cell drops from 10.85% to 6.58% being kept in ambient conditions (see Figure 3.14). After this, regular J-V measurements were done for next 90 days. As can be seen from the plot in Figure 3.14, the efficiency has stabilized after 40 days to ~5.7%. Oxidation of Si surface on Si-Ni interface is probable due to absence of Ni_2S layer which might be a possible reason for reduction in efficiency of the device. Bringing SiN_x layer for surface passivation over the Ni network can protect the device from oxidation ensuring its performance stability.

II. 5 Comparison of different metal wire networks on Ŝi solar cell

To fabricate top electrodes on Ŝi solar cell, in present work three metals are explored to serve as seed layer for top conducting Cu layer. All these metals are deposited by physical processes like thermal evaporation and sputtering. Sputtering is done only for Au due to lack of availability of the sputtering unit for other metals. As can be seen from the combined J-V plots in Figure 3.15, Ni enormously outperforms Au and Sn. All the cells in Figure 3.15 have used Ŝi solar cell 1 as the starting material. Au/Cu wire network performs reasonably well but its unfavorable interaction with Si reduces its efficiency with time. Sn as a seed layer for Cu is not effective enough because of diffusion of Cu into Si through it. Ni as a seed layer for Ni-Cu network on Si provides a good barrier to the Cu layer by forming Ni_2Si. As Ni wire network is chemically bonded to the Ŝi solar cell, it is likely that it has better adhesion compared to other metals. This might be the reason out its outstanding performance. Ni being a favorable metal for silicon solar cell proves to be a good top electrode having performed best when coated unaided.

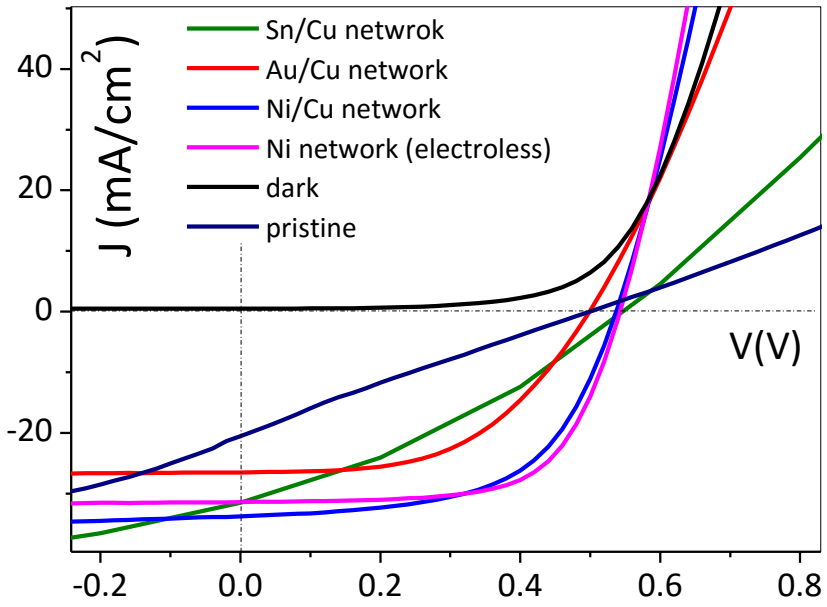

Figure 3.15 Comparison of J-V characteristics of different metal wire network brought on Ŝi solar cell 1 compared to pristine and dark.

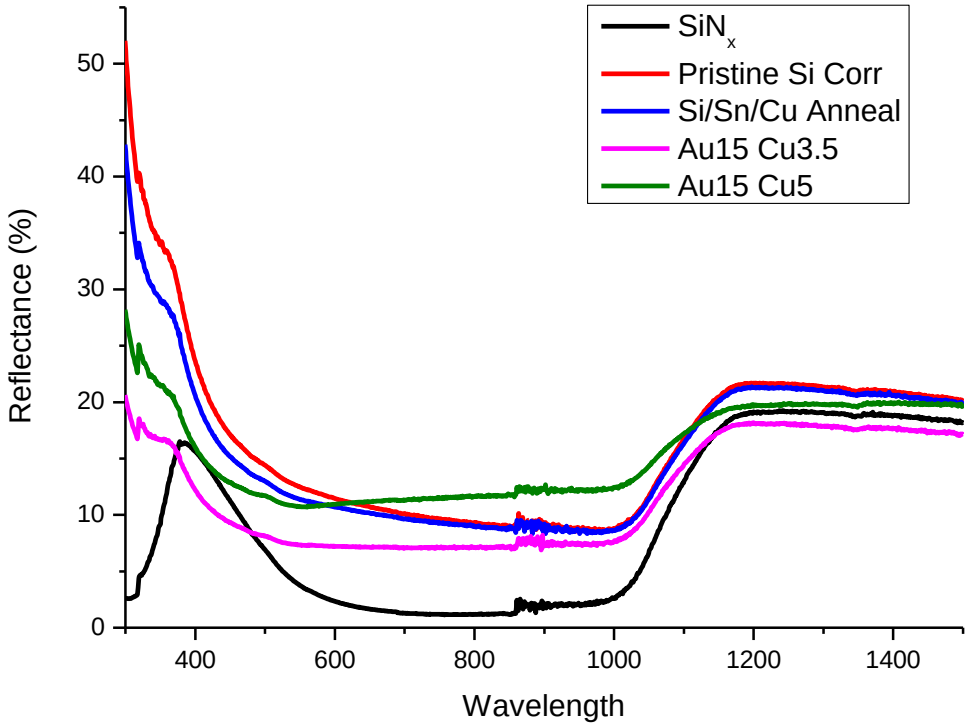

Figure 3.16 Reflectance spectra for Si doped/Corrugated samples with Au/Cu and Sn/Cu coated network in range 300nm to 1500nm and their comparison with SiN_x coated samples

Pristine Si has a reflection of ~30%. For that reason, surface of Si is made corrugated. The pyramidal texturing helps absorb more photons lowering it reflectance to 10%. As the reflection is due to free charge carriers inside Si, the surface requires an insulating anti reflecting coating on top such as SiN_x, MgF_2, ZnO etc. As SiN_x can be grown easily chemically on crystalline Si and is robust, it is most commonly used anti-reflecting coatings having reflection of only 2% except in the blue region (~400nm). In the present work, it was observed that the Au (15min.)/Cu (3.5min) network visibly reduces the reflectance of bare corrugated Si to 8%. The result was unforeseen as introducing a metal, ordinarily would lead to increased scattering and enhanced reflection which was clearly not the case here. The reflectance for this Au-Cu network solar cell was observed to be lesser than even SiN_x coated Si solar cell in the blue region. The reason for this might be less metallicity at such a small scale (refer to SEM images in Figure 3.6). Higher deposition of Cu increases the reflectance as can be seen for the green curve compared with pink curve (see Figure 3.16). Higher aspect ratio of metal may not affect specular reflection much but it greatly affects scattering from other angles. The reflectance results are in agreement with the efficiency results. The optimum Cu deposition on Ŝi solar cell/Au(15 min)-Cu(5 min) solar cell has the highest efficiency (6.89%) with minimum reflection (8%).

Part III. Commercial Si solar cell

Commercial Si solar cell, as is available in the market has two additional features compared to Ŝi solar cell. Along with pyramidal texturing, it has 100 nm thick SiN_x coating on top that acts an anti-reflection coating. The top electrodes are made by screen printing process in which Ag ink is fired into the SiN_x coated wafer covered by a mask. By this process, a 2 mm busbar of Ag is made along the diagonal of SiN_x coated Ŝi solar cell and fine Ag fingers are made perpendicular to the busbar at a separation of 3 mm with each other. Due to the firing of Ag ink, the Ag widens along its thickness from top to bottom. This causes shadowing of the Si wafer and hence less number of photons are absorbed by the cell. As these cells are readily available compared to Ŝi solar cells, the effects of bringing metal wire network on commercial Si solar cell were studied.

III.1 Commercial Si solar cell/Ag network

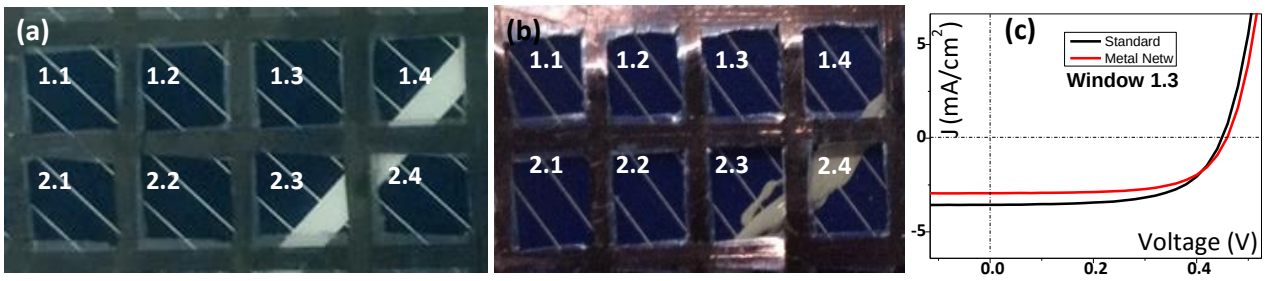

Figure 3.17 Study on Commercial Si solar cell before and after coating with Ag wire network in different windows. (a) Commercial Si solar cell covered by a mask having 8 squares each 0.16 cm^2 in area. (b) Commercial Si solar cell/Ag wire network covered by same mask as in (a). (c) J-V characteristics of Commercial solar cell in window 1.3 before and after coating Ag wire network.

About 1 mg of CP was dissolved in 1 mL thinner by ultra-sonication for 10 minutes and was spin coated on commercial Si solar cell (see Figure 3.17a) at 1000 rpm for 120 s. After spin coating, a crackle pattern was obtained on the solar cell such that crackle widths are smaller on Ag fingers compared to that on SiN_x regions. This

has happened because of lower thickness of CP on Ag fingers compared to SiN_x. Over this template, Ag was deposited by thermal evaporation and then CP was lifted off in chloroform. Figures 3.17a and b show commercial Si solar cell before and after coating with Ag wire network. The cells are covered by a mask having eight square windows marked 1.1 to 2.4. A cardboard with opening of same area as these windows was kept sequentially on these windows and J-V characteristics were recorded for all the windows before and after introducing Ag wire network for comparing in the corresponding regions. The efficiency of Commercial cell reduces after coating with Ag network but becomes more uniform all over as can be seen from the bar graphs shown in Figure 3.18b.

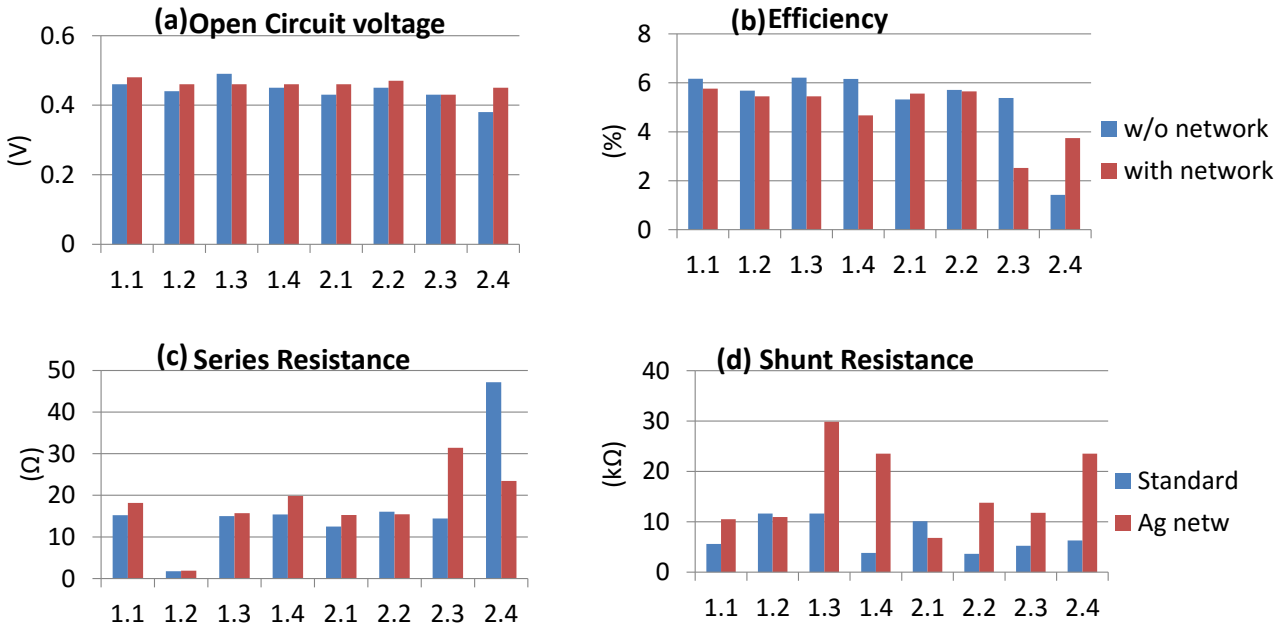

Figure 3.18 Comparison of Solar cell parameters before (blue) and after (red) coating with Ag wire network. (a) V_{oc}, (b) Efficiency, (c) Series Resistance and (d) Shunt resistance.

Among all the parameters, V_{oc} and Fill Factor FF increase after coating with Ag wire network in many windows (see Figure 3.18a and b). To analyze this, series and shunt resistance which affect the FF of the J-V curves, were calculated for J-V measurements in all the windows. To estimate series resistance, the inverse of slope of J-V curve at y-axis was calculated and for shunt resistance, the inverse of slope at

x-axis was calculated. The comparison of Series and Shunt resistance before and after introducing Ag wire network on top is shown by histograms in Figure 3.18c and d respectively.

III.2. Performance of Commercial Si solar cell with Ni wire network top electrode

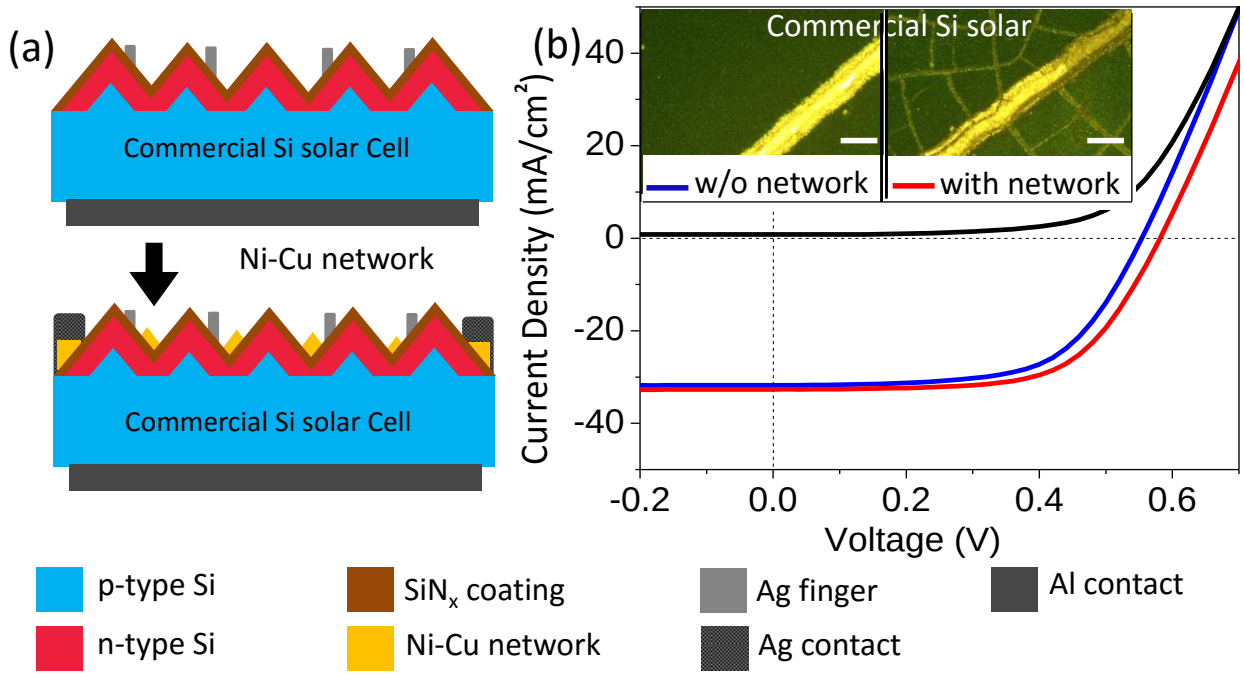

Figure 3.19 J-V characteristics of commercial Si solar cell. (a) Side view schematic of commercial Si solar cell before and after coating with Ni-Cu wire network. (c) J-V characteristics of commercial Si solar cell before and after coating Ni-Cu wire network compared with that of dark (black curve).(Inset) Optical micrographs of commercial Si solar cell with and without Ni-Cu network. White scale bar measures 100 µm.

After working with bare Si surfaces, commercial Si solar cell was used as a substrate to carry Ni/Cu wire network following the similar procedure as done for Ŝi solar cell. The side view of fabricated solar cell before and after coating with Ni-Cu wire network is shown in Figure 3.19a. The efficiency was expected to reduce because of increased shadowing of metal but surprisingly the efficiency enhanced from 10.89 % in the commercial cell to 12% in commercial cell with the introduction of Ni-Cu wire network as top electrodes (Commercial Si solar cell/Ni-Cu

network)(see Table 3.4). The diffusion length of charge carriers in Si is few hundreds of microns but the distance between the fingers of screen-printed electrodes is 3mm. The micron wide random crackle arrangement might have efficiently reduced the path travelled by charge carriers making recombination less probable leading to highly squarish J-V characteristic as shown in Figure 3.19b. Optical micrographs in the inset of Figure 3.19b clearly shows the minimization of finger width due to the random crackle network. The current collection becomes uniform and significant that no shadowing loss could be observed. As the commercial cell has SiN_x passivation coating on top, a possibility of pin holes in the coating is expected which are allowing the top seated Ni-Cu wire network to make contact with the underlying Si.

Table 3.4 Performance parameters of commercial Si solar cell with and without Ni-Cu wire network

Standard Si solar cell with Ag electrodes and SiN_x coating	Without Ni wire network		With Ni-Cu wire network	
Time in ambient conditions	As obtained	After 125 days	As prepared	After 125 days
Annealing time at 420 °C (s)	0	0	30	30
Cu electroless time (min)	0	0	5.5	5.5
Area (cm^2)	0.72	0.72	1.125	1.125
V_{oc} (V)	0.55	0.56	0.581	0.576
J_{sc} (mA/cm^2)	31.77	31.72	32.68	32.51
FF (%)	61.92	56.31	63.18	62.95
Efficiency (%)	10.89	10.05	12.01	11.79

III.3. Aging of Ni wire network on Commercial Si solar cell

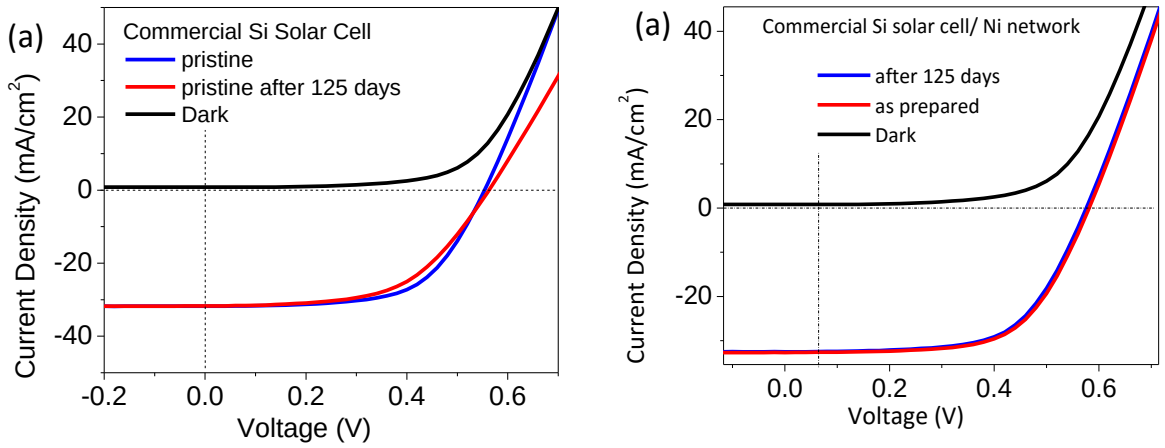

Figure 3.20 Aging of Ni wire coated Si solar cell. (a) J-V characteristics of commercial Si solar cell as obtained and after 125 days compared to dark. (b) J-V characteristics of commercial Si solar cell with Ni-Cu network as prepared and after 125 days compared to dark.

Commercial Si solar cell/Ni-Cu wire network showed an insignificant reduction in efficiency of 0.2% after keeping in ambient for 125 days (see Table 3.4), J-V curves are overlapping quiet well (see Figure 3.20b). The commercial cell without Ni network was observed to have degraded performance after 125 days as shown by J-V characteristics in Figure 3.20a. Ni wire network is most probably playing a role in improving the stability of commercial Si solar cell. Ni wire network can serve as a very promising top electrodes for Si solar cell if stability of the underlying substrate is ensured.

References

1. Li, Z.; Kulkarni, S. A.; Boix, P. P.; Shi, E.; Cao, A.; Fu, K.; Batabyal, S. K.; Zhang, J.; Xiong, Q.; Wong, L. H.; Mathews, N.; Mhaisalkar, S. G., Laminated Carbon Nanotube Networks for Metal Electrode-Free Efficient Perovskite Solar Cells. *ACS Nano* **2014,** *8* (7), 6797-6804.
2. Wang, X.; Zhi, L.; Müllen, K., Transparent, Conductive Graphene Electrodes for Dye-Sensitized Solar Cells. *Nano Letters* **2008,** *8* (1), 323-327.
3. Kulkarni, G. U.; Kiruthika, S.; Gupta, R.; Rao, K. D. M., Towards low cost materials and methods for transparent electrodes. *Curr Opin Chem Eng* **2015,** *8*, 60-68.
4. Raval, M. C.; Solanki, C. S., Review of Ni-Cu Based Front Side Metallization for c-Si Solar Cells. *Journal of Solar Energy* **2013,** *2013*, 20.
5. Kiruthika, S.; Gupta, R.; Rao, K. D. M.; Chakraborty, S.; Padmavathy, N.; Kulkarni, G. U., Large area solution processed transparent conducting electrode based on highly interconnected Cu wire network. *J Mater Chem C* **2014,** *2* (11), 2089-2094.
6. (a) Rao, K. D. M.; Hunger, C.; Gupta, R.; Kulkarni, G. U.; Thelakkat, M., A cracked polymer templated metal network as a transparent conducting electrode for ITO-free organic solar cells. *Phys Chem Chem Phys* **2014,** *16* (29), 15107-15110; (b) Rao, K. D. M.; Kulkarni, G. U., A highly crystalline single Au wire network as a high temperature transparent heater. *Nanoscale* **2014,** *6* (11), 5645-5651.
7. Gomezrodriguez, J. M.; Baro, A. M.; Salvarezza, R. C., Fractal Characterization of Gold Deposits by Scanning Tunneling Microscopy. *J Vac Sci Technol B* **1991,** *9* (2), 495-499.
8. Raval, M. C.; Joshi, A.; Solanki, C. S., Analyzing Impact of Background Plating from Alkaline Ni bath for Ni-Cu metallization. *Ieee Phot Spec Conf* **2013**, 2254-2256.

Chapter 4

Transferability of Au wire network on different substrates

Introduction

So far, metal wire network has been grown on a desired substrate by electroless or physical means and was used as an electrode for the same substrate. However, it was noticed that when the Au electroless deposition on Si was done for longer duration, the network starts detaching from the substrate and finally floats while lifting off the acrylic crackle layer. In this work, various methods of transferring Au wire network on to polymeric substrates were developed and studied to realize transparent conductors with good transmittance and conductivity.

I. Fabrication of Au wire network based transparent conductors

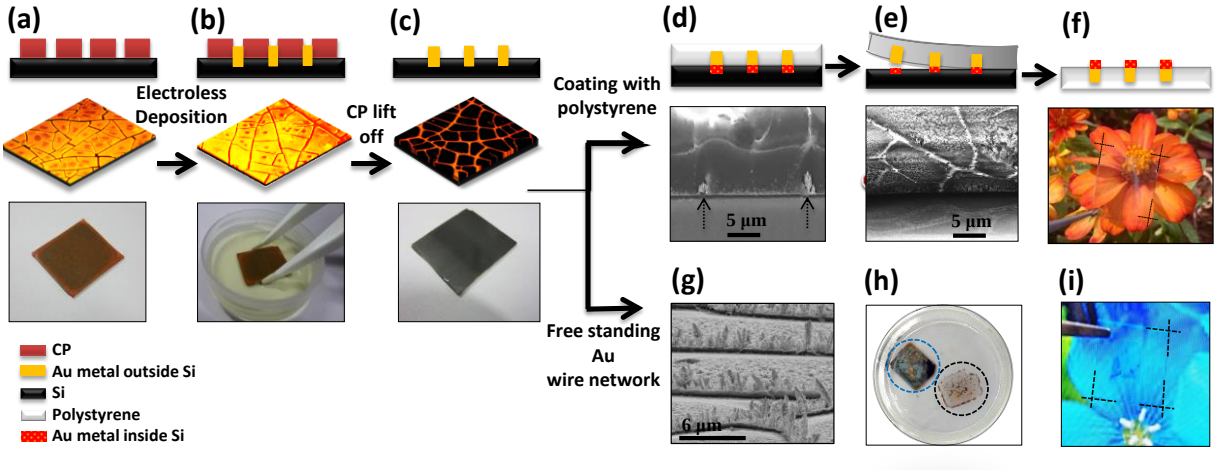

Figure 4.1 Process flow for transferring Au wire network. (a) coating of crackle based acrylic resin on Si wafer, (b) deposition of Au on CP coated wafer by electroless method, (c) lifting off the acrylic resin to get Au wire network on Si wafer, (d) coating of polystyrene on Au wire network containing Si wafer (cross-sectional SEM image at the bottom), (e) peeling away Au wire network embedded in polystyrene from Si wafer (cross sectional SEM image at the bottom), (f) Completely peeled off polystyrene film to get Au wire network based TCE, (g) Detaching of Au network from Si wafer helping it in freely standing, (h) Au wire network containing Si wafer immersion in water to get free standing Au wire mesh (Parent silicon wafer in blue circle and peeled off Au mesh in black circle), (i) transferring free standing network on a glass substrate (periphery of TCE marked with dashed black lines). In (a-c), top

panel shows the side view schematics, middle panel shows the dark field micrographs and bottom panel shows the digital camera images of corresponding stages.

A Si substrate was cleaned by ultra-sonication in acetone, IPA and water successively and then kept in UV-Ozone pro cleaner for 20 minutes to remove the native oxide layer. A crackle based colloidal solution was prepared in the concentration of 0.7 mg/µl and spin coated on the cleaned Si substrate at 1000 rpm for 60 s.[1] Figure 4.1a (top to bottom) shows the cross sectional view, dark field micrograph and digital image of Si substrate containing crackle pattern (CP). A 10 mM Au electroless solution was prepared by dissolving 17 mg $HAuCl_4$ in 3.9 mL water and dissolving 1.1 mL HF in it.[2] The CP coated Si substrate was then kept in Au electroless solution for 2 minutes to get Au deposited in cracks as depicted by three images in Figure 4.1b. After two minutes, the substrate was kept in DI water to remove any Au electroless solution traces and then kept in chloroform to dissolve the CP. The Au wire network on Si was obtained as explained by the Figure 4.1c.

Transferring Au network on Polystyrene

A 200 mg/mL solution of polystyrene in toluene was drop coated on the Au wire network containing substrate. This was then left for drying in ambient condition. The Au wires cutting at the cross-section (as shown by arrow marks) can be clearly seen in SEM image in the Figure 4.1d. The sample was then peeled from the Si wafer after immersing for 2 hours in water using forceps as shown in Figure 4.1e. The remnant mirror pattern of Au network on Si after peeling off polystyrene film (as shown in the SEM image) indicates that the metal network is not fully engulfed inside the polystyrene. This protruding of metal wire network out of the polymer film makes it conducting. During electroless deposition, the HF etches the exposed Si followed by Au deposition. When transferred on polystyrene, the part inside Si now comes at the top as marked in red color in Figure 4.1e. The polystyrene based TCE is transparent as observed by the digital camera image in figure 1f.

Making free standing Au wire mesh in water

To make the deposited Au wire network detach from the Si surface , the initial UV-Ozone cleaning step was skipped. This made the adhesion between Si and Au network weak which can be visualized by SEM image in Figure 4.1g. The CP deposited Si wafer was dipped in Au electroless solution for longer durations compared to polystyrene transfer to make it mechanically stable for freely standing. After rinsing in water, Au wire mesh coated Si wafer was dried using N_2 blower and kept in water. This made the Au wire mesh to float on water as shown in Figure 1h. The freely standing wire network was carried on a glass substrate for further characterization. A glass substrate was immersed in water and the Au wire mesh was lifted on to it so that the bottom surface of Au mesh (marked by red in schematic) now comes in contact with glass. On the other hand, to transfer on polystyrene, the polymer solution was dropped on the top surface hence exposing the bottom surface of Au wire mesh. A digital photograph of Au wire mesh on glass shows its highly transparent nature.

II. Fill Factor calculation of Au wire network.

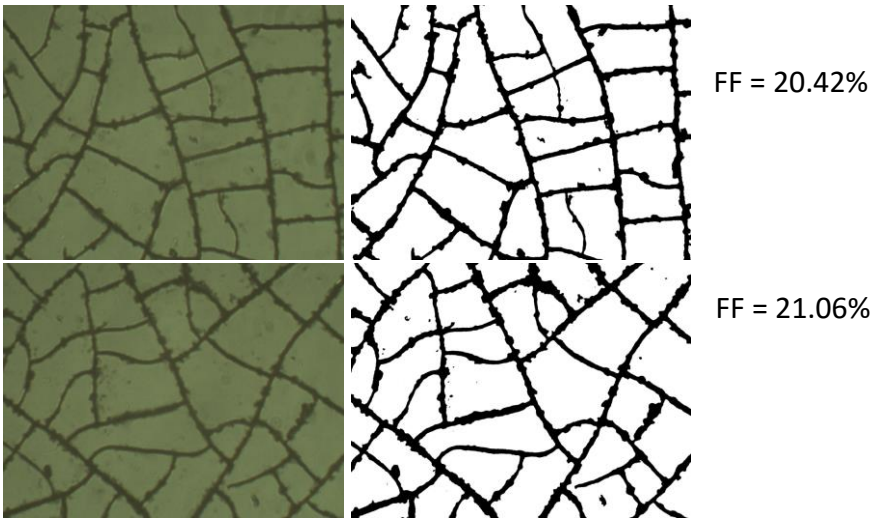

Figure 4.2 (a) Optical microscope image and (b) corresponding imageJ picture and FF calculation.

The optical micrographs of Au wire network were converted into Image J files (shown in figure 4.2) and fill factor was calculated by adjusting the contrast to the network regions. It was found that the Au wire network covers only ~21% area of the whole TCE. The fill factor is directly related to the crack width but does not vary with varying the amount of Au deposition. These networks have sheet resistance less than 10 Ω/□. The sheet resistance can be manipulated by changing the deposition time without affecting the transparency of the TCE.

III. Characterization of polystyrene embedded and freely standing Au wire networks

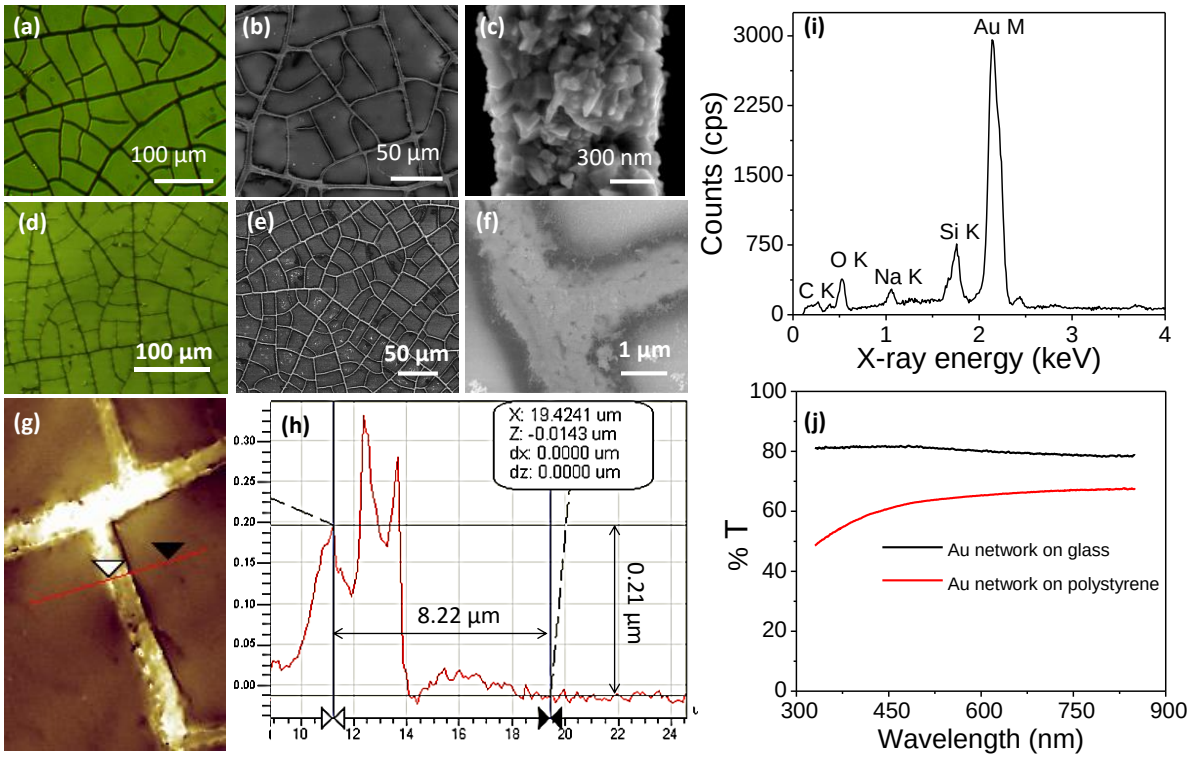

Figure 4.3 Characterisation of Au network based TCEs. (a) Optical micrograph, (b-c) SEM images of Free standing Au wire network taken on glass; (d) Optical Micrograph, (e-f) SEM images of Au wire network on polystyrene; (g) AFM image, (h) depth profile of Au network on polystyrene; (i) EDS spectrum of free standing Au wire network; (h) transmittance curves for free standing and polystyrene based TCE.

Unlike in the case of silver nanowire and carbon nanotube based TCE, transparency of Au network based TCE need not be compensated to lower its sheet resistance.

The free standing Au wire network was taken on a glass substrate and its transmission mode optical micrograph and Scanning Electron Micrographs (SEM) were recorded as shown in Figure 4.3(a-c). The surface of the free standing mesh is very rough due to particle by particle nature of electroless deposition technique. Similarly optical and SEM images were recorded for polystyrene based TCE. The optical images show high interconnectivity of the wires for both the transferring procedures. There is noticeable difference between the zoomed in SEM images for the two transferring procedures. When transferred on polystyrene, the Au metal inside the Si (marked by red in Figure 4.1d) comes at the top surface (see Figure 4.1f). On the other hand, while making the free standing Au wire network, the active deposition part outside the Si (marked by yellow in Figure 4.1d) comes at the top while transferring onto a glass substrate. This is the reason for more roughness in free standing Au wire network. The Au network on polystyrene was found to be 0.21 μm thick on an average as seen in the AFM image in Figure 4.3g. The freely standing

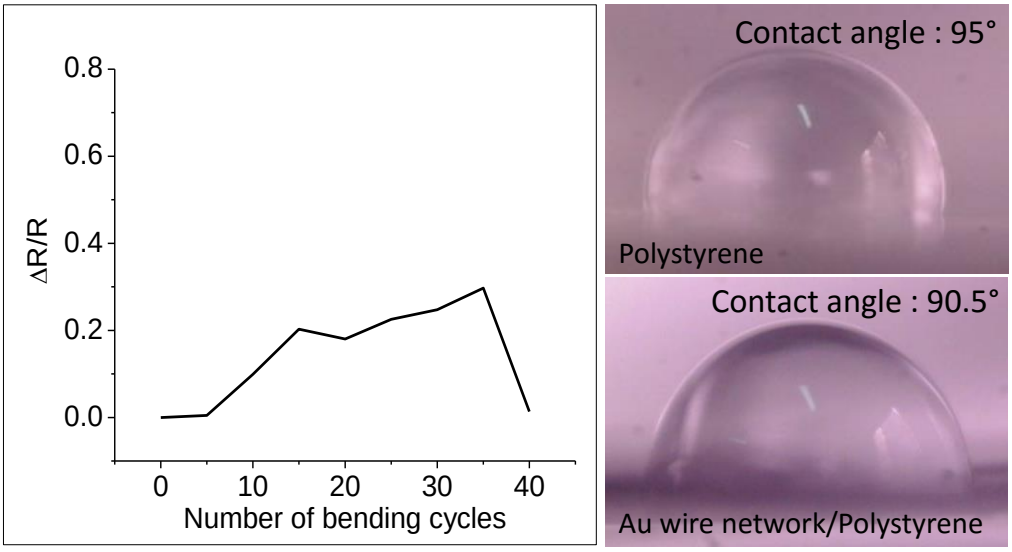

Figure 4.4. Flexibility and hydrophobic nature of TCE. (a) Relative change in resistance with number of bending cycles; (b) Contact angle of water droplet on polystyrene based TCE.

Au network has mettalic gold as shown by the EDS spectrum in Figure 4.3i. The Si peak has appeared because it was used as substrate to carry the Au mesh. Free standing network is 80% transmitting as shown in Figure 4.3j. Polystyrene based sample shows transmittance of 65% for a sheet resistance of 19Ω/□. The significant decrease in transparency is due to inherent nature of the polymer that it becomes milky on bending or stretching. For this reason, transferability of Au mesh was tried on other polymers also such as PMMA and PDMS.

IV. Properties of polystyrene based TCE

Bending tests were done on polystyrene based TCE for 40 cycles. As can be seen from the plot in Figure 4.4a, after some fluctuations the sheet resistance comes back to original value. This suggests that the network regains the connections once stress is released making the TCE flexible. The contact angle of water droplet was measured to be 90.5°. As compared to 95° on pristine polystyrene, it was seen that Au metal mesh sitting on the polymer minimally affects the hydrophobicity of the polymer.

V. Properties of free-standing Au network

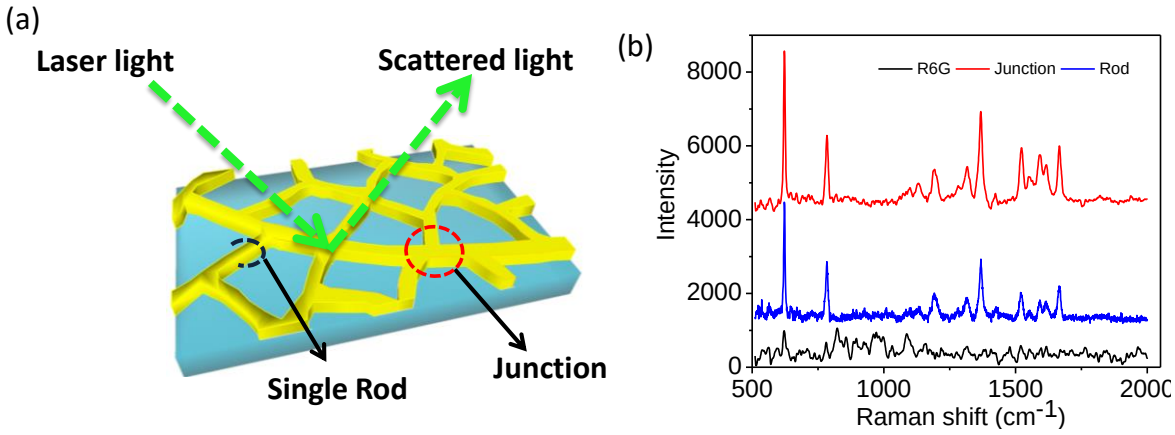

Figure 4.5 (a) Schematic showing laser focusing on Junction or rod of Au wire network of free standing network for SERS measurement. (b) Raman intensity of R6G at the rod and at the junction of the Au wire network.

To perform Surface Enhanced Raman Spectroscopy (SERS), commonly used sample for enhancement calculation, Rhodamine 6G dye was used.[3] The dye solution in water was drop coated on the Au wire network on Si. SERS was performed on the single rod and junction of the Au wire mesh schematically shown in the Figure 4.5a. From the plot in Figure 4.5b, it can be seen that, both the single rod and junction gave Raman intensity enhancement of the R6G. The Raman intensity at the junction shooted up even higher than that on single rod suggesting higher roughness in the former case.

VI. Transferability of Au wire network on other polymers

Au network on Si was used for transferring on many other polymers like PMMA, PVA and PDMS. A brief discussion on the realization of each transfer is explained here.

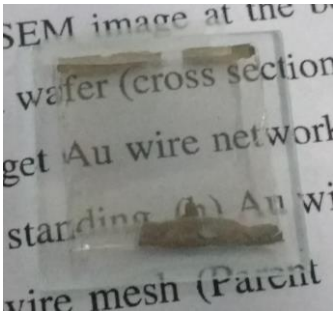

PDMS: Polydimethylsiloxane, a Si based organic polymer in its raw form is a highly viscous flowing liquid. To give structural rigidity, curing agent is added to it which acts as cross linkers of polymer chains. The cured PDMS is a highly flexible and optically transparent solid. Typically to make a PDMS mould, the raw PDMS is mixed vigorously with the curing agent in the ratio 10:1 in a plastic container.[4] Then, this mixture is desiccated for 20 minutes to remove the air bubbles and to form completely clear liquid. This liquid is then kept in a plastic mould at 80 °C for 40 minutes to cure. To transfer Au wire network from Si to PDMS, Au film was grown on two edges of the Si wafer and then two dots of Ag paste were put at the interface of Au network and Au film on both the sides. The PDMS and curing agent mixture was poured onto this and kept for curing. The Au edge films and Ag dots helped the Au wire network not to get completely embedded. When the Si wafer having Au network was used without Au edge films and Ag dots, the network got completely

embedded in the polymer making it non-conducting. The Au side pads prevent the network to get completely engulfed by PDMS and remain exposed at the surface. After curing, the PET on the back side was removed and the Si wafer was peeled off fast to ensure maximum transfer of Au wire network from Si to PDMS.

Poly(methyl methacrylate), PMMA is another polymer which was used to make Au network based TCE. 3 g PMMA power was dissolved in 100 mL acetone by sonicating in a closed vial for 1 h.[5] 1 mL of this solution was drop coated on the Au wire network coated Si wafer. This was left for drying in ambient conditions till the solvent evaporated completely. Then the PMMA coated Si wafer was immersed in water for peeling off similar to the step in case of polystyrene. The PMMA layer peeled off with the Au network just with one prick of the forceps unlike Polystyrene, which had to be manually peeled from all the corners. Also, PMMA TCE was more robust as compared to Polystyrene as it did not bend creating milky areas. Therefore, it was expected that PMMA would give rise to more transparent TCEs as compared to polystyrene with the similar Au wire network.

Polyvinyl Alcohol (PVA) is a water soluble polymer. This polymer was also used to make Au wire network based TCE. To dissolve in water, ~30 mg of polymer was put in 5 mL DI water and stirred with the help of magnetic bead. After 10 minutes, another 30 mg PVA was poured in the stirring solution. The steps were repeated 10 times to get a thick solution.[6] The solution was prepared by gradually adding PVA in water because if all the amount was added at once, the PVA forms a lump preventing the core of particles to be dissolved. This solution was drop casted on the Si wafer containing Au wire network. It was kept in ambient conditions for 24 h to dry all the water. Then this PVA coated Si wafer with Au network was immersed in Toluene to separate the PVA film from Si. The PVA film did not get separated even after manually trying to peel from all the corners. PVA was found to have stronger adhesion to Si as compared to other non-polar polymers.

References

1. Kiruthika, S.; Rao, K. D. M.; Ankush, K.; Ritu, G.; Kulkarni, G. U., Metal wire network based transparent conducting electrodes fabricated using interconnected crackled layer as template. *Materials Research Express* **2014,** *1* (2), 026301.
2. Gupta, R.; Rao, K. D. M.; Kulkarni, G. U., Transparent and flexible capacitor fabricated using a metal wire network as a transparent conducting electrode. *Rsc Adv* **2014,** *4* (59), 31108-31112.
3. Li, P.; Zhou, X.; Liu, H.; Yang, L.; Liu, J., Surface-enhanced Raman evidence for Rhodamine 6G and its derivative with different adsorption geometry to colloidal silver nanoparticle. *Journal of Raman Spectroscopy* **2013,** *44* (7), 999-1003.
4. Meitl, M. A.; Zhu, Z.-T.; Kumar, V.; Lee, K. J.; Feng, X.; Huang, Y. Y.; Adesida, I.; Nuzzo, R. G.; Rogers, J. A., Transfer printing by kinetic control of adhesion to an elastomeric stamp. *Nat Mater* **2006,** *5* (1), 33-38.
5. Xue, F.; Fu, W.; Cheng, R., Characterization of Acetone-Solution Casting Film of PMMA. *Frontiers of Chemistry in China 1* (1), 45-47.
6. Hassan, C. M.; Trakampan, P.; Peppas, N. A., Water Solubility Characteristics of Poly(vinyl alcohol) and Gels Prepared by Freezing/Thawing Processes. In *Water Soluble Polymers: Solutions Properties and Applications*, Amjad, Z., Ed. Springer US: Boston, MA, 2002; pp 31-40.

Chapter 5

Summary and Future Outlook

In this work, it was demonstrated that metal wire networks can be conveniently fabricated in ambient conditions using electroless deposition. The networks can be coated conformally on highly rough surface of Si solar cell with minimal shadowing effects. Among all the metals explored, Ni proved to be most inexpensive, stable and easy to fabricate top electrodes for Si solar cell. The solution processed Ni wire network when brought on to pristine Si solar cell without silver electrodes significantly increased its efficiency from 2.79% to 11.15%. Commercial Si cells when coated with Ni-Cu wire network showed enhanced performance with efficiency increasing from 10.89% to 12.01%. After Ni wire coating, the commercial solar cell was stable for longer time compared to that without network.

Another interesting feature of the metal wire network is its adaptability to transfer on to any substrate from the one on which it was grown. It was found that PDMS, PMMA and polystyrene based transparent conductors can easily be prepared by transferring Au wire network from Si substrate where it was electrolessly grown. The polystyrene based transparent conductor was found to be flexible and hydrophobic having 65% transmittance for a sheet resistance of 19 Ω/□. Free-standing Au mesh was made and found to be highly transparent with transmittance of 80%. This free standing network can be used for making any poorly conducting surface into highly conducting just by placing the network onto chosen surface. The surface can be of any shape and size; not necessarily planar. The free standing Au network due to its high surface roughness showed better surface enhanced Raman scattering (SERS) compared to polished Si wafer.

However, stability of the Ni wire electroless coated corrugated p-n junction Si solar cell without SiN_x coating decreases with time. This can be resolved by coating the device with passivation layer like SiN_x by PECVD or a protective coating to prevent oxidation. Also by depositing Ni via sputtering instead of thermal evaporation can provide better contacts with Si as sputtering involves partial

implantation of active metal into the target substrate. New methods of fabrication can be explored in which the metal network locally reaches the Si substrate in presence of SiN_x coating. This can be a significant step in fabricating low cost Si solar cells.